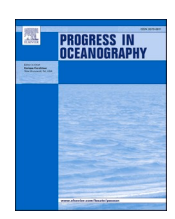
ELSEVIER

Contents lists available at ScienceDirect

Progress in Oceanography

journal homepage: www.elsevier.com/locate/pocean



Dispersal pathways of European green crab larvae into and throughout the eastern Salish Sea

Jiabi Du ^a, Carolyn K. Tepolt ^b, Emily W. Grason ^c, P. Sean McDonald ^d, Yan Jia ^b, Weifeng G. Zhang ^{b,*}

- ^a Department of Marine and Coastal Environmental Science, Texas A&M University at Galveston, TX, USA
- ^b Woods Hole Oceanographic Institution, Woods Hole, MA, USA
- ^c Washington Sea Grant, University of Washington, Seattle, WA, USA
- d Program on the Environment & School of Aquatic and Fishery Sciences, University of Washington, Seattle, WA, USA

ABSTRACT

The invasive European green crab (*Carcinus maenas*) was first detected on the US west coast around 1989 and has expanded its range northward from central California to southern Alaska. The eastern Salish Sea was initially thought to be protected from invasion by the dominant seaward surface current in the Strait of Juan de Fuca (SJdF). However, this "oceanographic barrier" has been breached as established green crab populations have been detected in the eastern Salish Sea in recent years. Here we carried out particle-tracking simulations to understand possible natural pathways of green crab larvae invading the eastern Salish Sea. Both diel vertical migration and temperature-dependent mortality were considered in these simulations. Our results suggest that green crab larvae from the outer coast (outside the Salish Sea) and Sooke Basin (in SJdF) could be carried into the eastern Salish Sea in a narrow time window during the later cold season (esp. in March) when frequent flow reversals in SJdF occur and the seasonally rising water temperature becomes relatively favorable for green crab larvae. The major pathway for larvae to reach the eastern Salish Sea is along the southern coast of SJdF. The probability of live larvae reaching the eastern Salish Sea is highly sensitive to water temperature. Sensitivity simulations indicate that a temperature increase of 0.5–1 °C would double or quadruple the probability of successful arrival in the eastern Salish Sea. This suggests that invading green crabs might have taken advantage of the mild winter conditions in recent warm years. Our results also suggest that the warming climate in the near future may facilitate green crab larval exchange across the Salish Sea.

1. Introduction

Relative to terrestrial or freshwater systems, marine species invasions are generally more difficult to predict and control, both because of the large geographic scale on which they occur and the highly open and connected nature of marine environments. In addition, many marine invasive species have a highly dispersive larval stage that can spend weeks or months in the plankton, making flow-mediated dispersal a major factor in their spread (Kinlan and Gaines, 2003; Palumbi and Pinsky, 2014). Dispersal patterns of marine species, which are a product of the interaction between local oceanographic processes and the biology and behavior of the species (Alvarez-Noriega et al., 2020; Morgan et al., 2021), affect all stages of invasions, from arrival through establishment, spread, and impact (Cowen and Sponaugle, 2009). Prearrival, the complexity and scale-dependent variability of oceanographic processes can result in diverse and cryptic pathways for movement of marine species. Post-arrival, the most likely source of regional spread is often assumed to be the nearest known population, but hydrographic connectivity could weaken the correlation between distance and dispersal probabilities (Kinlan et al., 2005) and enable unintuitive invasion trajectories. Ocean modeling is a powerful tool that can reveal important pathways and barriers to dispersal both in space and time, generating management-relevant insight into regional population dynamics.

Using a modeling approach, this study aims to characterize the hydrographic processes that could have facilitated recent spread of the larvae of invasive European green crabs (*Carcinus maenas*, hereafter referred to as "green crab") in the eastern Salish Sea. The green crab, native to northwestern Europe and Africa, is considered one of the most damaging invasive species globally (Ens et al., 2022). Green crab can survive in a wide range of environmental conditions, and are highly eurythermal (Weihrauch and McGaw, 2023). They can tolerate short-term exposure to extreme conditions, including water temperatures from 0 to 35 °C, though the minimum temperature is 10 °C for growth and 7 °C for feeding (Berrill, 1982; Klassen and Locke, 2007). The species has successfully established non-native populations in Australia and

^{*} Corresponding author at: 266 Woods Hole Road, WHOI, MS#11, Woods Hole, MA, 02543, USA. *E-mail address:* wzhang@whoi.edu (W.G. Zhang).

Tasmania, South Africa, Argentina, Japan, and both coasts of North America (Carlton and Cohen, 2003; Hidalgo et al., 2005). Green crabs have caused long-term degradation of eelgrass habitats and have negatively impacted bivalve, native crab, and finfish populations in their invasive ranges (see reviews by Grosholz and Ruiz, 1995; Ens et al., 2022).

Green crabs first became established in the US on the east coast near Long Island Sound, New York by 1817 (Carlton and Cohen, 2003). Their population on the US west coast is believed to have spread from an initial introduction discovered in San Francisco Bay in 1990 (Cohen et al., 1995; Grosholz and Ruiz, 1995). Since then, the species has steadily expanded its range northward on the west coast, facilitated by the Davidson Current (Behrens Yamada et al., 2021a, 2021b). Currently, green crabs are found as far north as Metlakatla, Alaska, where they were first detected in August 2022 (Alaska Department of Fish and Game Press Release #22–3413). Northward larval dispersal is stronger during years with positive Pacific Decadal Oscillation (PDO) and El Niño Southern Oscillation (ENSO) indices (Behrens Yamada and Kosro, 2010). During the 1997-1998 ENSO, green crab populations were first detected in estuaries on the outer coast of Washington, Oregon and British Columbia (hereafter referred to as outer ocean coast). Shortly after that, they became well-established in several of the fjord-like inlets on the west coast of Vancouver Island.

For more than a decade following regional expansion on the west coast of the US and Canada, no population was found within the inland waters of British Columbia (BC) and Washington State (WA), known as the Salish Sea, which is connected to the North Pacific Ocean by the Strait of Juan de Fuca (SJdF) in the west and Johnstone Strait in the north. This changed in 2012, when a well-established green crab population was detected in Sooke Basin on Vancouver Island, BC (a bay on the north coast of SJdF; Fig. 1) (Curtis et al., 2015). This population was apparently isolated to that basin, which has only limited connectivity to the SJdF, and likely resulted from human-mediated transport of mussels for biotoxin monitoring. The first detection in the eastern portion of the Salish Sea occurred at the San Juan Islands, WA, in 2016 (Grason et al., 2018). Green crabs have since patchily established at several other sites along the SJdF and eastern Salish Sea, and since 2019, they have been consistently present at low populations at a growing number of locations in the eastern Salish Sea (Keller et al., 2022), prompting the development of large scale management efforts.

The SJdF was initially believed to serve as a natural oceanographic barrier preventing eastward spreading of green crab larvae (Grason et al., 2018; Brasseale et al., 2019). The Salish Sea can be considered as a large estuary with the SJdF being the mouth (Giddings and MacCready, 2017). Under normal conditions, including in the upwelling season, circulations in the SJdF exhibit a pattern of estuarine exchange flow with a westward outflow at the surface and eastward inflow at depth (e. g., Cannon, 1978; Frisch et al., 1981; Holbrook et al., 1980; Thomson et al., 2007). The surface outflow layer on average occupies the top 50-80 m (Giddings and MacCready, 2017), much thicker than the 3-15 m depth range green crab larvae inhabit over the course of observed diel vertical migration (DiBacco and Therriault, 2015). The surface outflow under normal conditions thus tends to suppress eastward transport of coastal larvae toward the eastern Salish Sea. However, during downwelling seasons, under the influence of winds and the Columbia River plume, the exchange flow in SJdF can reverse occasionally, becoming inward at the surface and outward at depth (e.g., Hickey et al., 2009; Holbrook and Halpern, 1982; Thomson et al., 2007). These flow reversals occur mostly in fall and winter (Frisch et al., 1981; Giddings and MacCready, 2017) or during short-term storm events (Behrens Yamada et al., 2017), and they can enable eastward advection of green crab larvae.

Ongoing genetic analysis suggests the populations in the eastern Salish Sea are a mixture of Sooke Basin origin and outer ocean coast origin (CK Tepolt, unpublished data). Based on the locations where green crabs are currently found, these populations are not likely to have

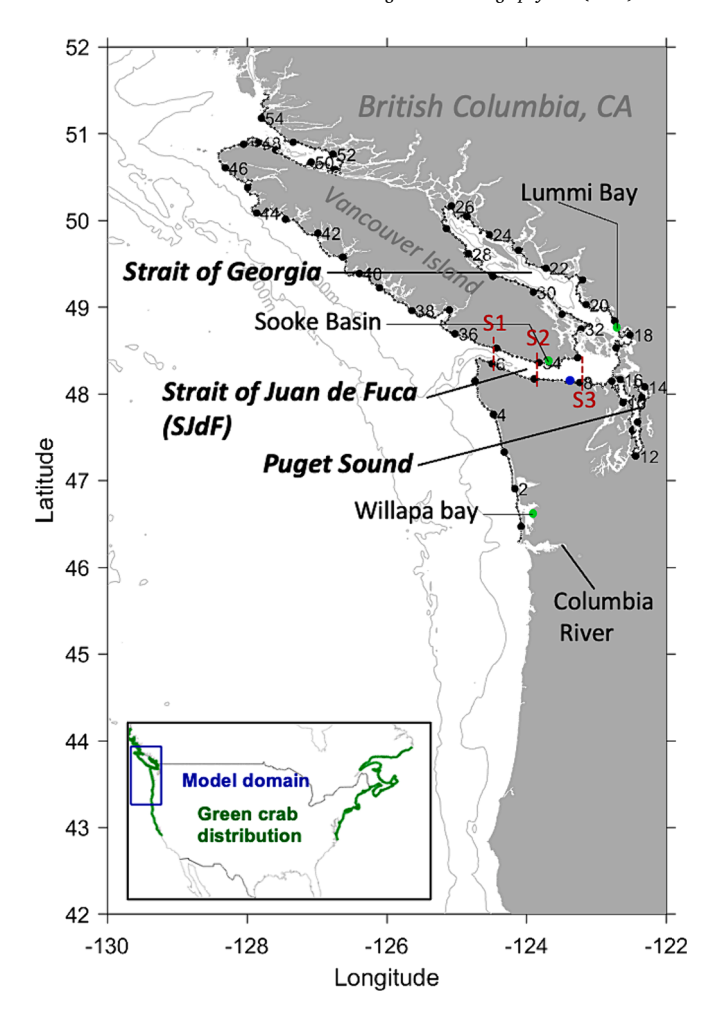


Fig. 1. Regional map showing the Salish Sea and the coastal region off Oregon, Washington, and British Columbia. The domain of the LiveOcean model is shown by the blue rectangle in the inset; the particle release locations, i.e., Sooke Basin, Lummi Bay (a representative eastern Salish Sea site), and Willapa Bay, are marked by green dots; the small black dots are evenly distributed sampling locations on the coast where possibility of released particles reaching different sections of the coastline is calculated; the large black dots and the corresponding indices represent some selected sampling locations and provide reference positions; the red dashed lines across Strait of Juan de Fuca indicates three cross-channel sections where velocity data are analyzed. The blue dot on the south shore of SJdF indicates the location of Port Angeles, where continuously measured water temperature is examined. The green lines in the inset highlight currently known distribution of green crabs within the continental US and Canada, excluding Alaska. (For interpretation of the references to color in this figure legend, the reader is referred to the web version of this article.)

resulted from human-mediated transport, raising the question of whether and how natural transport processes in the ocean, such as the occasional flow reversals in the SJdF, may have facilitated the expansion of green crabs into the eastern Salish Sea.

Previous efforts have been made to understand the transport of green crab larvae in the region using Lagrangian particle tracking models coupled with hydrodynamic models (e.g., Banas et al., 2009; Brasseale et al., 2019). Aiming to understand the sources of the initial invasion to the south side of the SJdF and eastern Salish Sea from 2014 — 2016, Brasseale et al. (2019) conducted particle tracking simulations to examine possible transport pathways of green crab larvae. Diel vertical migration (DVM) of the particles was included in their model. They found that particles released on the outer ocean coasts (outside the Salish Sea) both to the north and south of the SJdF mouth could reach the eastern Salish Sea. Building on this prior work and using the same

hydrodynamic model (McCready et al. 2021), we implement an additional factor influencing green crab larval dispersal, temperature-dependent larval mortality, to quantitatively examine possible direct pathways of green crab larvae reaching farther eastward into the eastern Salish Sea in 2017–2020, covering the more recent expansion of the population in the region in 2019. The emphasis of this study is on the statistically most likely pathway of green crab larval transport to the eastern Salish Sea, and its temporal and spatial variability.

Along with access to suitable habitat at developmental competence, water temperature is likely one of the most important environmental conditions that determine the success of larval dispersal (O'Connor et al., 2007). The largest range expansions of green crab on the US west coast occurred during the last two major El Niño periods during which water temperature in the region was abnormally high (see Section 4). During the 1997-1998 El Niño, green crabs colonized embayments on the coasts of Oregon, Washington, and Vancouver Island; during the 2015-2016 El Niño and marine heatwave period, green crabs first invaded the Salish Sea outside of Sooke Basin (Behrens Yamada et al., 2021a, 2021b). Given this, we hypothesize that water temperature exerts a strong influence on the spread of green crab larvae into the eastern Salish Sea. The impact of water temperature is considered in this study by incorporating the influence of temperature-dependent larval mortality in the particle tracking model. The influence of seasonal temperature variation and potential future warming on live green crab larval spread in the eastern Salish Sea is also analyzed in the context of understanding persistence and expansion of green crab in the region in a warming world.

2. Method

2.1. Hydrodynamic and Lagrangian particle models

An offline Lagrangian model built on top of a realistic hydrodynamic model is used in this study. The realistic hydrodynamic model, i.e., the LiveOcean model (Giddings et al., 2014; Giddings and MacCready, 2017; MacCready et al., 2021), provides hydrodynamic fields for a domain covering the Salish Sea and the coastal ocean off Oregon and Washington in the US, and Vancouver Island, British Columbia in Canada. The LiveOcean model, based on the Regional Ocean Modeling System (ROMS) (Haidvogel et al., 2000; Shchepetkin and McWilliams, 2005), has a model grid with 500 m spacing in most of the Salish Sea and Washington coastal estuaries, and the grid stretches up to 3 km at open boundaries. The model has 30 vertical terrain-following layers. The model is forced by discharges of 45 rivers, 8 tidal constituents, open ocean conditions from a global data-assimilative model, and atmospheric forcing from a regional weather forecast model. The LiveOcean model has been extensively validated against observations, which shows that the model generally captures i) coastal ocean variability induced by Columbia River plume, coastal-trapped waves, and wind-driven upwelling and downwelling (Giddings et al., 2014), ii) exchange flows in the SJdF (Giddings and MacCready, 2017), and iii) salinity and stratification variations in Puget Sound (MacCready et al., 2021).

The Lagrangian particle-tracking package, ROMSPath (Hunter et al., 2022), is used to simulate the direct transport and survival probability of green crab larvae. Built upon the Lagrangian transport (LTRANS) model (North et al. 2008), ROMSPath calculates particle trajectories using a fourth-order Runge-Kutta ordinary differential equation solver on the native ROMS grid, which is advantageous in the handling of velocity interpolation, land-sea masking, and boundary interaction, and thus provides more accurate results. Moreover, ROMSPath enforces a kinematic boundary condition of no flow across the coastline or seafloor, which prevents particles from passing through land cells. In this study, 3-dimensional (3D) hourly velocity field from the LiveOcean model is used to drive the ROMSPath calculation of particle trajectories with a time step of 60 s. In simulations without DVM, particles are advected in the water column by the modeled 3D velocities. In simulations with

DVM, particles are fixed at a predetermined depths (see below) and only experience velocity at those depths.

2.2. Biological attributes

In this study, besides the dispersal of particles by ocean circulation and mixing, we also consider the influence of two biological attributes of green crab larvae, namely DVM and temperature-dependent mortality. These attributes are implemented in the ROMSPath particle-tracking model. To distinguish between simulations conducted with and without these biological attributes, in this work, we refer to the modeled particles without any biological attributes as *particles*, and the ones with biological attributes as *simulated larvae*.

As part of DVM, green crab larvae tend to stay subsurface (typically above the pycnocline) during daytime and migrate to the surface during nighttime. DVM is commonly believed to be a strategy for predation avoidance (Vaughn and Allen, 2010). Plankton surveys at Barkley Sound by DiBacco and Therriault (2015) revealed a notable vertical difference in the abundance of Stage I zoeal larvae of green crab, which were nearly absent at the surface during daytime but abundant in the nighttime. The weighted mean depths for Stage I zoeae at Barkley Sound were 1.5-1.9 m shallower during nighttime when compared to daytime (the pycnocline depth is about 2 m in Barkley Sound). In this study, following Brasseale et al. (2019), DVM is implemented by fixing the particles at 15 m below surface during daytime and 3 m below surface during nighttime with instantaneous changes of depths at sunrise and sunset as determined by local short-wave solar radiation. This simplification avoids complications in particle tracking modeling (Visser, 1997; Banas et al., 2009).

Mortality of green crab larvae can also greatly affect their dispersal. To consider its impact on the invasion process, temperature-dependent larval mortality as measured by de Rivera et al. (2007) is implemented in the model. Based on lab experiments, de Rivera et al. (2007) used a polynomial function to depict the larval survival rate (i.e., 1 - mortality rate) as a function of temperature. To avoid a negative survival rate in the lower temperature regime given by the polynomial function, we use a Gaussian function to parameterize the impact of temperature on zoeal survival rate at each moment during larval development (Fig. 2). Another reason to use a Gaussian function is the fact that larvae have higher physiological tolerances to temperature fluctuations than adults and can survive after being exposed to low temperature for only a short period of time (Dawirs et al. 1986; de Rivera et al. 2007). The Gaussian function of the larval survival rate used in this study is

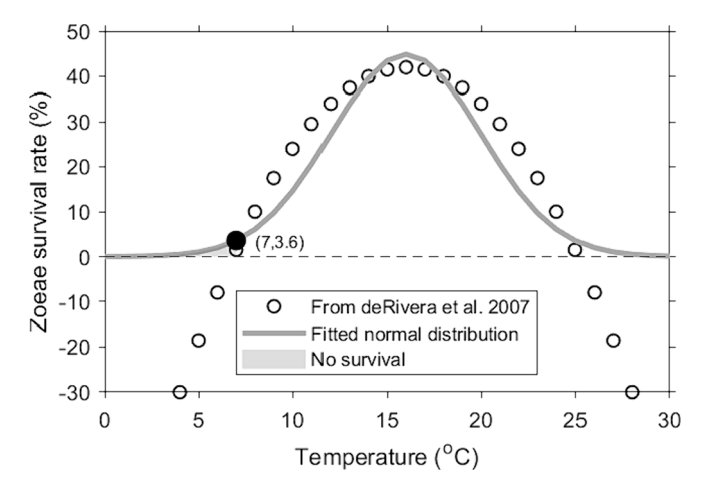


Fig. 2. Fitted Gaussian distribution of the larval survival rate (line) and the polynomial survival rate function (black open circles) from de Rivera et al. (2007). The solid black circle represents a critical condition for larval survival at the minimum constant temperature of $7\,^{\circ}$ C.

$$f(T) = Ce^{\frac{1}{2}\left(\frac{T-\mu}{\sigma}\right)^2} \tag{1}$$

where T is temperature, and C, σ , and μ are all constants, representing a scale of the maximum survival rate, a representative scale of the habitable temperature range, and the temperature of maximum survival rate, respectively. To reproduce the polynomial curve from de Rivera et al. (2007), we choose C=0.45, $\sigma=4$ °C, and $\mu=16$ °C (Fig. 2). Note that f(T) is the percentage of larvae that successfully complete their development if placed in an environment with a constant temperature of T. The duration of the larval development period varies with temperature, and we here use a typical duration, D=30 days, based on the laboratory study by de Rivera et al. (2007). The survival rate after each model time step, Δt , is thus,

$$g(T) = e^{\left[\frac{\log f}{D/\Delta I}\right]} = f^{\frac{\Delta f}{D}} = C^{\frac{\Delta f}{D}} e^{-\frac{\Delta f}{D}\left(\frac{T-\mu}{\sigma}\right)^2}$$
(2)

The survival of larvae is implemented in the model by adding a property to the particles, h, which could be considered a larval health index. The initial value of h is set to 1. To represent mortality, h decreases at each time step at a rate determined by the local temperature-dependent survival rate, g(T). Because f < 1, h can only decrease with time. That is, the decrease of h accelerates under non-favorable temperature conditions (too hot or too cold), and h does not recover even if the temperature that the simulated larvae experience becomes more favorable later. To quantify the probability of simulated larvae surviving at a specific location, we define the survival probability of a particle at any time as

$$P = max\left(0, \frac{h - f(T_{min})}{1 - f(T_{min})}\right) \tag{3}$$

Here, following de Rivera et al. (2007), we choose a minimum constant temperature of survival, $T_{min} = 7^{\circ} C$. That is, when $h < f(T_{min}) = 0.036$ (i. e., 3.6 % of its initial value), the survival probability is 0. To be

consistent with the findings of Dawirs et al. (1986) and de Rivera et al. (2007), we design the formula in (3) to allow simulated larvae survive after being exposed to temperature less than T_{min} for only a relatively short period. P can be interpreted in two ways: 1) the survival probability of an individual larva at a given time if each particle represents a single larva, and 2) the percentage of larvae surviving at a given time if a model particle represents a larval population. The survival probability is greatly influenced by the water temperature, and simulated larvae released in cold vs. hot seasons will differ substantially in their survival probability. For instance, a larva released at Sooke Basin in January 2017 will have its survival probability become zero on day 30 after release, while its survival probability will be 20 % after 30 days if it is released in July 2017 at the same location (Fig. 3).

2.3. Numerical experiments

Particles are continuously released at three shallow near-shore locations, namely, the mouth of Sooke Basin (on the northern side of the SJdF), the mouth of Willapa Bay (on the Washington coast outside of the Salish Sea), and a region immediately to the west of Lummi Bay (in the eastern Salish Sea). These three locations represent local concentrations of high relative abundance of adult green crabs and possible influential sources of green crab larvae to the eastern Salish Sea (Keller et al., 2022). Willapa Bay has a well-established green crab population with genetic characteristics representative of those on the outer ocean coast and distinct from the Sooke Basin population (CK Tepolt, unpublished data). Note that Lummi Bay is in the middle of a new green crab hotspot in the eastern Salish Sea, and it is selected as an example to investigate possible future expansion of the green crab population in the region.

At each of the release sites, 48 particle release simulations are carried out across 4 years (2017–2020), one for each month. Each of the simulations is run for 120 days with 9 particles released at 1 m below surface and 9 particles released at 1 m above seabed every hour in the the first 30 days. Note that all release sites are less than 10 m deep. There are thus 12,960 particles being released in each simulation. Prior work in a

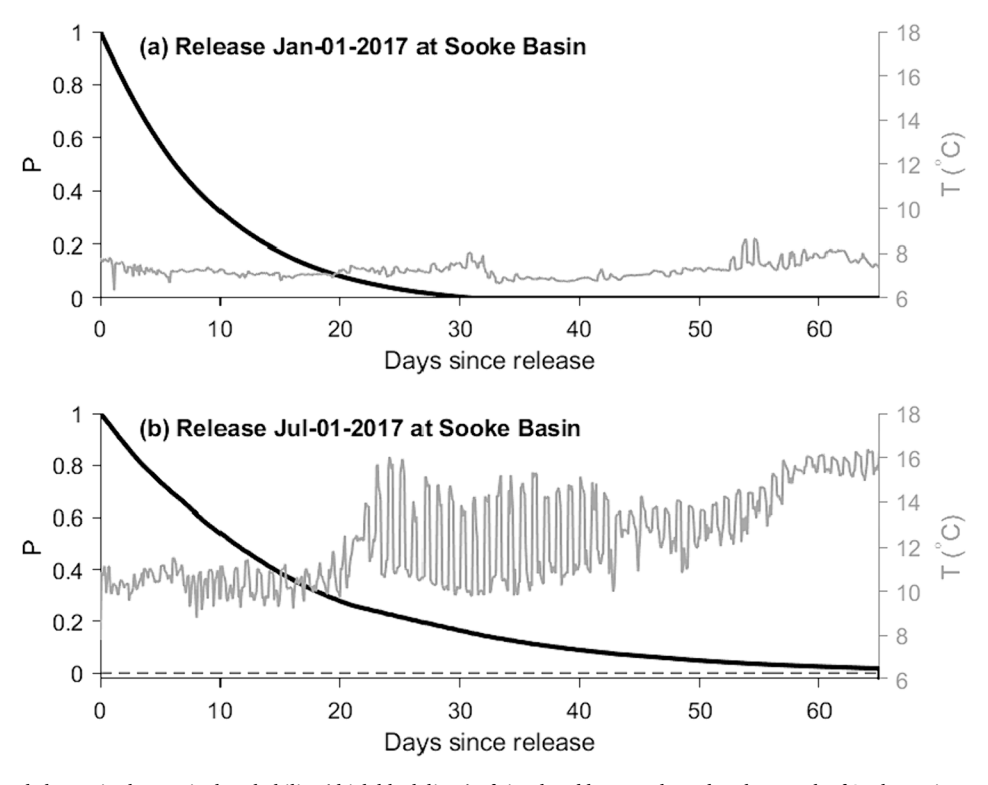


Fig. 3. Simulated temporal change in the survival probability (thick black lines) of simulated larvae released at the mouth of Sooke Basin on January 1 (top) and July 1 (bottom) 2017, and the water temperatures the simulated larvae experience (gray lines).

British Columbia inlet suggested that green crab spawning happens year-round, but has strong seasonal variation with most of the larvae being released in April-September (DiBaccio and Therriault 2015). However, a robust quantification of the seasonality of green crab larval release is lacking for many other sites, including the newly-established Salish Sea populations. We thus choose to focus on the influence of seasonal variation of the physical environment on larval dispersal patterns in this study, and here we have held the number of simulated larvae released in different times of the year constant. This caveat should be kept in mind when interpreting the simulation results, especially those related to the seasonality of larval dispersal.

To develop a first-order prediction of possible influences of ocean warming on larval dispersal patterns in the Salish Sea, we carry out sensitivity simulations with artificially increased water temperatures. In these sensitivity simulations, water temperature everywhere in the model domain is increased by 0.5 °C and 1 °C. These are typical temperature changes in the Salish Sea in the spring and fall seasons given by regional ocean simulations forced by downscaled future climate forcing representing the 21st century A1B greenhouse gas emissions scenario (Moore, et al., 2015). The A1B is a medium–high emission scenario reflecting 'business as usual' in the first half of the 21st century and greater mitigation in the second half (Nakicenovic et al., 2000).

2.4. Quantitative analysis

To quantify the success of larvae directly spreading to target regions, we introduce a success probability index, *S*, which is the mean survival probability of simulated larvae reaching a target area at a larval age of 30–75 days:

$$S = \frac{1}{N} \sum_{i=1}^{N} P_i$$
 (4)

Here, N = N(x, y, dx, dy) is the total number of particles reaching the target area during an age of 30–75 days; (x, y) is the coordinate of the center of the target area; dx and dy are the side length of the rectangular target area in the x and y directions, respectively; P_i is the survival probability of particle i reaching the target area for the first time. In this study, we choose $dx = 0.05^{\circ}$ in longitude (\sim 3.8 km) and $dy = 0.05^{\circ}$ in latitude (\sim 5.5 km). The age limits of 30 and 75 days are used to reflect realistic lower and upper bounds of the larval development period in the species, which has experimentally been measured as spanning from 31.5 days at 18 °C to 62 days at 12 °C at constant temperatures (Tepolt, 2023).

The success probability index provides a quantitative measure of how likely simulated green crab larvae are to be delivered from a release location to target regions. For example, S=1/1000 means that after releasing 1000 simulated larvae at a location, only one survives the journey reaching the target area in the model. S is influenced by not only the larval transport pathways but also the environmental conditions the larvae experience during transport. A larger value of S indicates that either the target location is more easily reached by larvae or the survival rate of arriving larvae is higher.

To understand how different coastal populations are connected through physical transport processes, we calculate the probability of simulated larvae from our three focal sites successfully dispersing to a range of sites along the shoreline. We focus on nearshore success probability because larvae must complete development and settle in the nearshore environment (Queiroga and Blanton, 2005). Larvae dispersed to open water regions are thus neglected in this analysis. To examine connectivity, we select 544 nearshore sampling stations that are spaced every 5 km along the shoreline from the outer southern coast of Washington to the coast in the Salish Sea and then the outer northern coast of Vancouver Island (large and small black dots in Fig. 1). A simulated larva is considered to have reached a station if it is within 2.5 km of the sampling station. At each station, the mean success probability of all

simulated larvae within a 2.5 radius is calculated. For visualization purposes, we averaged the success probability every 10 stations, resulting in a total of 54 major stations. The major sampling station indices increase to the north on the outer coast and in the anticlockwise direction within the Salish Sea (see station numbers in Fig. 1).

3. Results

3.1. Seasonal changes in the regional surface circulation

Flows in the SJdF are strongly sheared in the vertical direction with near-surface flows in the top $\sim 50~\text{m}$ being generally in the same direction and strongly influenced by winds and river plumes (e.g., Huyer et al., 1979; Thomson, 1981; Giddings and MacCready, 2017). As near-surface flows in the SJdF are a major driver of larval dispersal in the Salish Sea, we first describe seasonal variation in the modeled surface circulation in the strait, which is consistent with the flow pattern described in the aforementioned literature. Throughout the warm season (e.g., July), due to continuous injection of freshwater from rivers such as the Fraser and Skagit Rivers, surface salinity in the eastern Salish Sea is lower than in the open ocean (Fig. 4b). The outward flow of low-salinity Salish Sea water toward the ocean drives a persistent westward surface flow over most of the SJdF (Fig. 4b and 5). As a consequence, salinity in the SJdF gradually increases toward the west (Fig. 4b).

In wintertime, winds in the region are strong and generally southeasterly. Through onshore Ekman transport, the downwelling-favorable winds push outflow from rivers, such as the Columbia River, against the Oregon and Washington coast. The river plume then flows northward along the outer coast, forming a buoyant coastal current. During the winter-spring transition period (e.g., March), the combination of freshet-induced large river discharge and the downwelling favorable winds results in a strong northward buoyant coastal current. Essentially, under the influence of Coriolis and winds, the coastal current follows the coastline and flows in the same direction as the phase propagation of coastal-trapped waves. As it reaches the SJdF, where the coastline turns sharply right at the NW edge of the Olympic peninsula, the coastal current turns right and flows into the strait (Giddings and MacCready, 2017). Consequently, surface flows in part of the strait become eastward, forming so-called flow reversal (Fig. 4a and 5a). On the western end of the SJdF, strong flow reversals mostly occur on the northern side of the strait in winter and spring (Fig. 5b). In the central part of SJdF, strong flow reversals mostly occur on the southern half of the strait in fall and winter (Fig. 5c). On the eastern end of SJdF, flows are almost always westward throughout the year, except in narrow regions on the northern and southern coasts (Fig. 5d). These narrow flow reversals on the southern coast mostly occur in winter and spring. To carry green crab larvae eastward directly from the outer coast into the eastern Salish Sea, a journey of over 100 km, the flow reversal has to be continuous over the entire length of the strait. For this direct transport, the eastward tidally averaged flow must be strong enough (>0.03 m/s) to allow the larvae to reach a destination in the eastern Salish Sea during their planktonic stage of about 30 days. Considering all the cross-strait sections in Fig. 5 together, the necessary continuous and strong flow reversals in the SJdF occur once or twice a year, mostly in the winter months and lasting for 2-3 months, as highlighted by black ellipses in Fig. 5b.

3.2. General dispersal pattern of Sooke Basin larvae

Modeled distribution of dispersal exhibits a pronounced seasonal variation in all regions highlighted in this study (the outer coastal ocean, the SJdF, and the eastern Salish Sea), mostly consistent with seasonal variation in ocean circulation discussed above. Here, we first use the Sooke Basin release experiments to demonstrate the seasonal variation of particle distribution. We take an incremental approach and first examine the distribution of particles released at Sooke Basin without

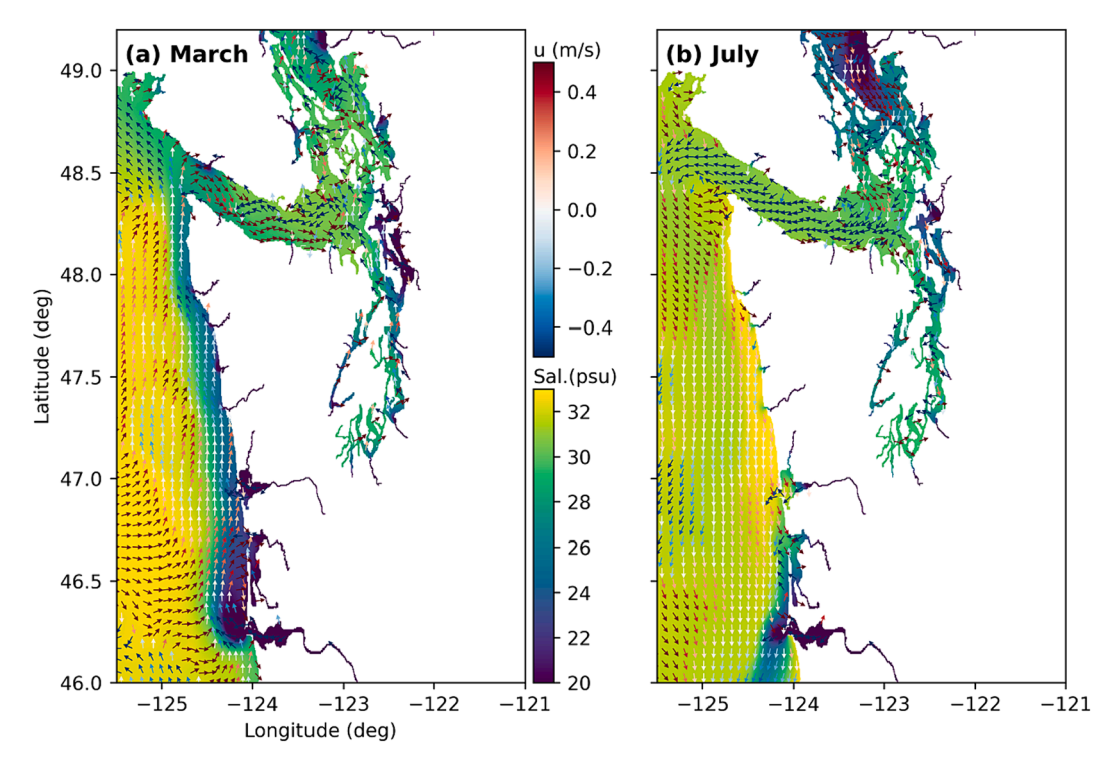


Fig. 4. Monthly mean surface salinity (blue to yellow color) and current (colored arrows) in the Salish Sea and adjacent shelf in (a) March and (b) July 2017. Red arrows indicate eastward velocities and blue arrows indicate westward velocities. (For interpretation of the references to color in this figure legend, the reader is referred to the web version of this article.)

considering the influence of DVM or temperature-dependent mortality (Fig. 6). This simulation captures the influence of ocean circulation on the particle dispersal without considering the interaction of circulation with DVM. A monthly climatology based on averaging the four modeled years shows that, throughout the year, a significant portion of the particles released at Sooke Basin are carried westward onto the outer shelf by the dominant westward flow in the SJdF. Seasonal distribution of modeled mean particle density on the outer shelf is consistent with a predominantly northward current in winter and southward current in summer on the continental shelf (Fig. 6). Consistent with the persistent westward current in the SJdF, an extremely low percentage of particles released at Sooke Basin during summer (June-August) reached the eastern Salish Sea. Due to the frequent flow reversals in the SJdF in winter months, a small portion of the particles released in November-March reach the eastern Salish Sea by developmental competence (30 days after release).

For the subsequent analysis, we examine the probability of simulated larvae reaching different locations in the model domain computed from the modeled particle trajectories. When temperature-dependent mortality and DVM are considered, the probability of simulated larvae released in Sooke Basin successfully spreading onto the outer shelf remains very high in the summertime (Fig. 7). This is because the high water temperatures during this time allow most of the larvae carried there by the westward current in the SJdF to survive. In the winter months, westward spreading of the simulated larvae is dramatically reduced because the low water temperature greatly increases larval mortality. Meanwhile, the eastward spread of the larvae in winter months is also reduced due to high mortality. From December to February, eastward spread is negligible with a success probability less than 210⁻³, primarily because of persistently low water temperatures around 7 °C in the Salish Sea (Fig. 8a). However, during transition months, e.g., March, April, October, and November, when water temperature is slightly higher than the minimum survival threshold, a small portion of simulated larvae is carried to the eastern Salish Sea with a success probability of 0.5–1.510⁻².

Further analysis suggests that the modeled success probability for simulated Sooke Basin larvae reaching the eastern Salish Sea is highest when they are released in March and November (Fig. 8d). This can be attributed to the combined effect of episodic current reversal in the SJdF and the slightly warmer water temperatures allowing some larvae to survive the journey. If temperature-induced mortality is ignored, up to 75 % of particles released in March at the mouth of Sooke Basin can reach the eastern Salish Sea at least once during the simulation period of 120 days. Considering only those larvae that reach the eastern Salish Sea between age 30 and 75 days, the maximum success probability reduces to ~ 2 % in March and November. When considering both the age requirement of 30-75 days and temperature-dependent mortality, the success probability becomes much lower, as shown in Fig. 7, because of high mortality during cold months. Water temperature at Port Angeles (at the southern coast of the SJdF; Fig. 1) generally reaches its minimum of \sim 7 $^{\circ}$ C in mid-February, resulting in high larval mortality in the simulations. In March and November, water temperature at Port Angeles is typically ~ 8 °C (Fig. 8a), which allows a small portion of the larvae to survive.

To further examine the role of DVM in these dispersal patterns, we carry out simulations with temperature-dependent mortality, but not DVM, in representative months. Note that, in the simulation without DVM, simulated larvae are advected in the water column by the 3D model velocity. However, because they are all released in the top 10 m and the vertical velocity in the model is not strong, most of them remain in the top 15 m over the course of the simulations. On average, 62 % and 65 % of the simulated larvae released in March and July 2017 remained in the top 15 m of the water column, respectively. Comparison of these new simulations with the previous simulations show that DVM of larvae affects their dispersal pattern in the warm season, but not in the cold season. For instance, simulated larvae released in Sooke Basin in March 2017 without considering DVM have a similar distribution as those with DVM (Fig. 9). However, larvae released in July 2017 without DVM are much more concentrated in the coastal region than those with DVM. This seasonal difference in the impact of DVM is consistent with the fact

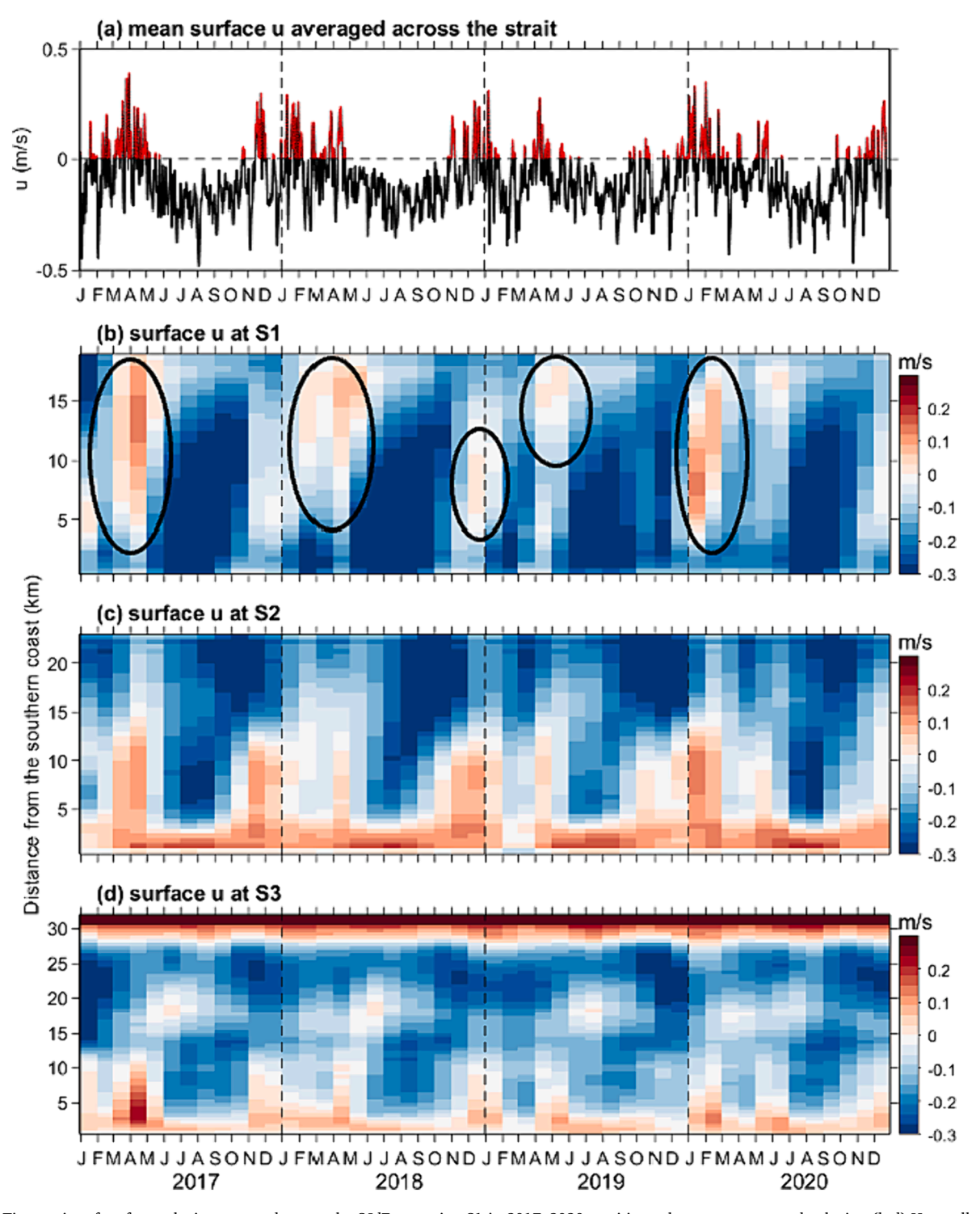


Fig. 5. (a) Time series of surface velocity averaged across the SJdF at section S1 in 2017–2020, positive values mean eastward velocity; (b-d) Hovmoller diagram showing cross-channel and temporal variations of monthly averaged, surface eastward velocity at Section (b) S1, (c) S2, and (d) S3. In (a), the black line depicts subtidal velocity smoothed with a running 50-hour window; the red lines highlight the eastward subtidal flows. In (b), black ellipses highlight episodic reversals of surface velocity in the strait with monthly mean eastward velocity greater than 0.03 m s^{-1} . Locations of the cross-channel sections are shown in Fig. 1. (For interpretation of the references to color in this figure legend, the reader is referred to the web version of this article.)

that the upper part of the water column is relatively well mixed in the cold season but stratified in the warm season. Thus, the flows simulated larvae experience at different depths in the top 15 m do not vary much vertically in cold months, but do vary vertically in warmer months. As the eastward transport of larvae toward the eastern Salish Sea occurs mostly at times of cold water temperatures, the effective impact of DVM on eastward transport is small.

3.3. Dispersal pattern of Willapa Bay larvae

Simulations of particles (without DVM or temperature-dependent mortality) released at Willapa Bay on the outer ocean coast also show a strong seasonal variation in dispersal: no particles released at Willapa Bay during the warm months, May-September, reached the eastern Salish Sea, while a small portion of the particles released in October-

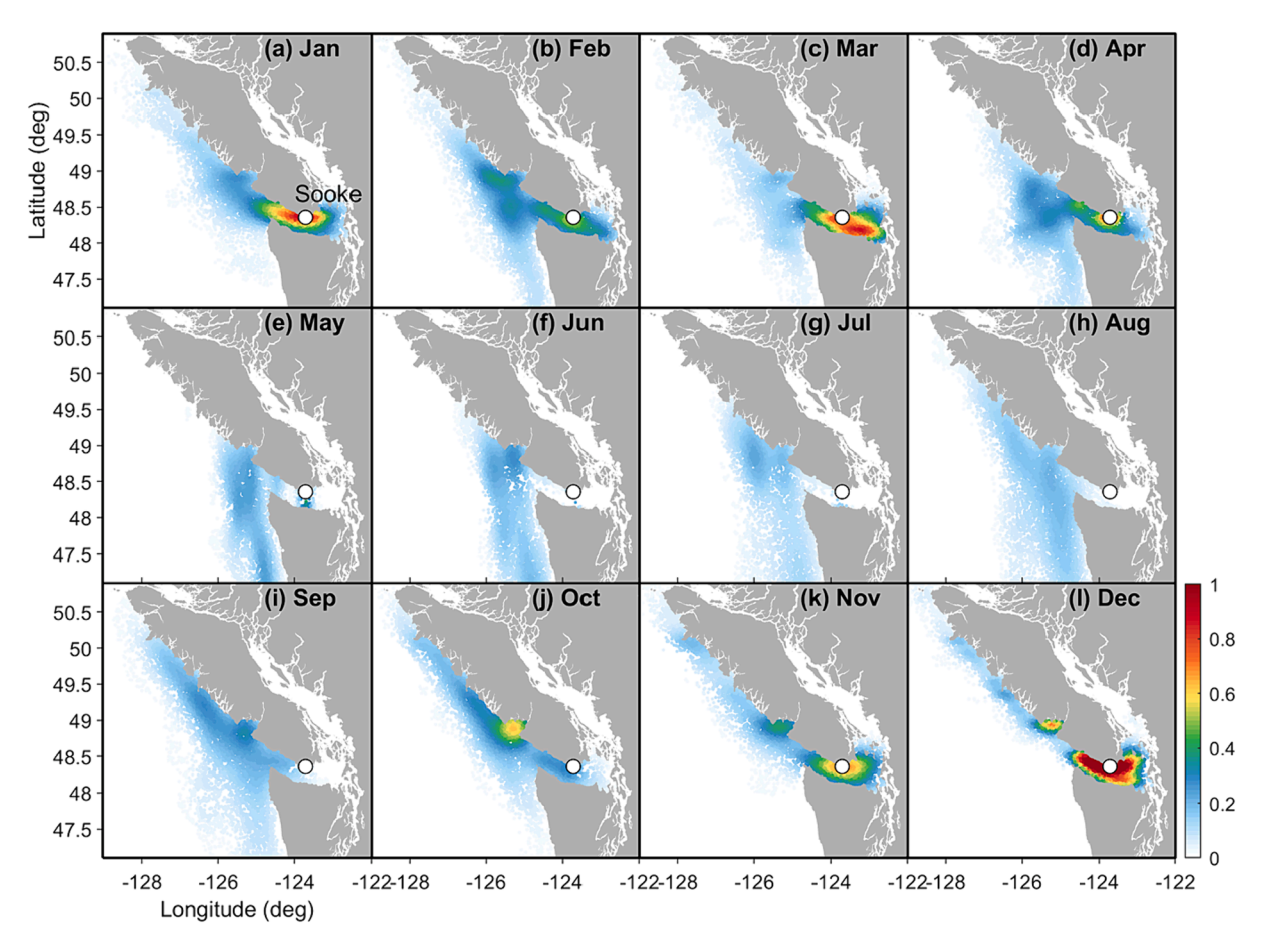


Fig. 6. Scatter plot showing the mean density of particles (no DVM or temperature-dependent mortality) 30 days after being released in each month at Sooke Basin. Color denotes the relative density of particles at each data point calculated with Kernel Density Estimate (Nils, 2023), a spatial smoothing estimate method for probability density. Each panel shows an average over all releases in the same months in 2017–2020. The release location is marked with a circle.

March did (Fig. S1). When temperature-dependent mortality and DVM are considered, the dispersal pattern of simulated larvae released at Willapa Bay is similar to that of the Sooke Basin larvae (Fig. 10). This is because particles released at both Sooke Basin and Willapa Bay are subject to the same current conditions in the SJdF and the eastern Salish Sea. Both Sooke Basin and Willapa Bay larvae tend to intrude into the eastern Salish Sea along the southern side of the SJdF. As described above (Fig. 5), current reversal occurs more frequently along the southern side of the strait. While the flow is generally moving westward when averaged across the channel, cross-channel variations of the flow could favor the eastward intrusion of green crab larvae from the coastal population. This general pattern of flows in the SJdF also helps to explain the comparable success probability of larvae released from both Sooke Basin and Willapa Bay invading into the eastern Salish Sea even though Willapa Bay is much further away.

Comparison of the simulations with and without DVM (with temperature-dependent mortality) in representative months show that DVM of larvae in the top 15 m does not qualitatively affect their overall dispersal pattern in the outer ocean and SJdF either in the warm or cold seasons (Fig. S2). This likely results from the surface mixed layer in the outer ocean being deeper than 15 m throughout the year, so the modeled DVM does not significantly alter the flow conditions larvae experience.

3.4. Dispersal pattern of Lummi Bay larvae

When released immediately to the west of Lummi Bay within the eastern Salish Sea, particles without DVM or temperature-dependent mortality disperse widely in both the central part of the east Salish Sea and the SJdF in all seasons (Fig. S3). In most months, a small portion

of the particles reach the outer coast, particularly the southwest coast of Vancouver Island. When DVM and temperature-dependent mortality are considered, the simulated larvae remain widely distributed in the warm months, but their spread is greatly suppressed in the cold winter months (Fig. 11). Note that modeled success probability of expansion in the eastern Salish Sea remains less than $0.2x10^3$ for simulated larvae released in December-February, because water temperature in the region is colder than 7 °C and larvae die out quickly. Meanwhile, the Lummi Bay population does not appear to be able to spread effectively to the northern Georgia Strait, particularly to the region north of the Fraser River. This is caused by the Fraser River plume that prevents northward transport of the larvae released in Lummi Bay. It is notable that southward dispersal is also greatly restricted – very little advection into Puget Sound or Hood Canal was observed over the four-year period. This results from the predominantly northward flow in Puget Sound in the model. Note that the model resolution is not high enough to resolve flow variability in narrow channels in Puget Sound, which likely affects simulated larval dispersal pattern there.

Simulations without DVM but with temperature-dependent mortality in March and July show geographically similar dispersal patterns in the Salish Sea to those in simulations with both DVM and temperature-dependent mortality (Fig. S4). In July, when the upper water column in the Salish Sea is highly stratified, simulated larvae without DVM released from Lummi Bay have an increased success probability in the SJdF and outer ocean relative to those where DVM is considered. This is consistent with the shallow surface mixed layer in the Salish Sea creating vertical shear in the horizontal velocity in the upper water column in the warm season.

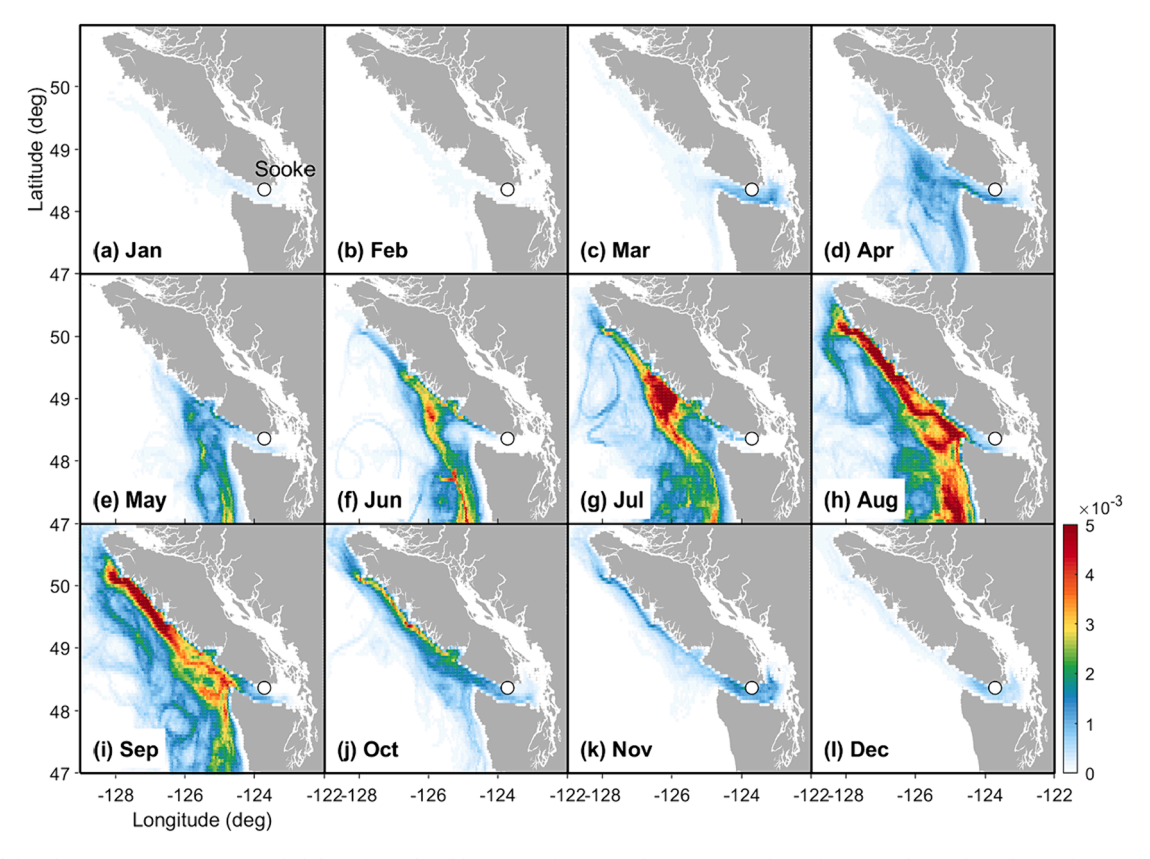


Fig. 7. Spatial distribution of mean success probability of simulated larvae (with DVM and temperature-dependent mortality) released in each given month at Sooke Basin. Each panel shows an average of all releases in the same months in 2017–2020. The release location is marked with a circle.

3.5. Larval connectivity

The computed connectivity map (Fig. 12) demonstrates that hot spots of success probability vary with release location and time. The Sooke Basin release experiments (Fig. 12) show that the southwestern coast of Vancouver Island receives the most simulated larvae throughout the year, while only larvae released from Sooke in April through October can reach the outer Washington and Oregon coasts. Meanwhile, simulated larvae from Sooke Basin can only reach the central part of the eastern Salish Sea in limited periods of the year, primarily March and November. Results of the Willapa Bay release experiments show that most simulated larvae disperse to the outer Washington and Oregon coasts throughout the year, with modest levels of larval success probability in the central part of the eastern Salish Sea in March, October and November (Fig. S5). Results of the Lummi Bay release experiments show the highest larval success probability in the nearby eastern Salish Sea region in relatively warm months (March – November) (Fig. S6). In the warmest months, simulated larvae from Lummi Bay can go through the SJdF and reach the outer Washington and Oregon coasts and the south coast of Vancouver Island.

A time series of the success probability indices shows details of the seasonal and interannual variability in the dispersal pattern of larvae released at the three sites. Larvae released at Sooke Basin tend to aggregate along the northern outer coast of Vancouver Island, while having little success in reaching the Georgia Strait and Puget Sound (Fig. 13a). Between June and October, some of the simulated Sooke larvae move southward, and many of them reach the southern coast of the SJdF. This larval dispersal pattern also varies from one year to another. For instance, the northward spread of the larvae released at Sooke Basin is much more successful in 2018 and 2019 than in 2017 and 2020; and the spread of these larvae to the outer southern coast was more successful in 2019 and 2020 than in 2017 and 2018. Meanwhile, a small portion of the simulated larvae could reach the Georgia Strait in

2017 and 2019, but were completely absent from this region in 2020. This results from the weaker and shorter flow reversals in the SJdF in spring 2020, compared to 2017 and 2019 (Fig. 5a).

Larvae released at Willapa Bay can reach sites on the southern outer coast throughout the year, but they can reach sites on the northern outer coast only in October to April (Fig. 13). This is consistent with seasonal variation in the circulation on the outer shelf (see below). There is also interannual variability in the northward spread of these larvae, which was much stronger in 2017 and 2018 than in 2019 and 2020. Meanwhile, larvae from Willapa Bay can reach the Salish Sea but concentrate along the southern side of the SJdF during most months, except in the summer (June-August). Larvae from Willapa Bay can even intrude into the Georgia Strait occasionally, for example, in November-December 2017 and December 2018. This is largely consistent with interannual variability of the eastward spread of larvae from Sooke Basin.

The Lummi Bay release experiments show a hotspot in a relatively small coastal region to the immediate north of Lummi Bay in the warm season of April to November in all four years (Fig. 13c). Some of the larvae from Lummi Bay can reach both sides of the SJdF and even disperse to the outer coast in the warm season of every year. In the cold seasons, the larvae do not spread anywhere because water in the eastern Salish Sea is too cold for them to survive. This is different from the other two release sites where wintertime water temperature is slightly warmer, allowing at least some potential year-round dispersal. Interestingly, the larvae from Lummi Bay do not reach the northern Georgia Strait or Puget Sound in any season. This is caused by the circulation in the northern Salish Sea being mostly southward and the circulation in Puget Sound being mostly northward in the warm seasons. Thus, the population in Lummi Bay is more likely to export larvae to the SJdF and the outer coast than to Puget Sound.

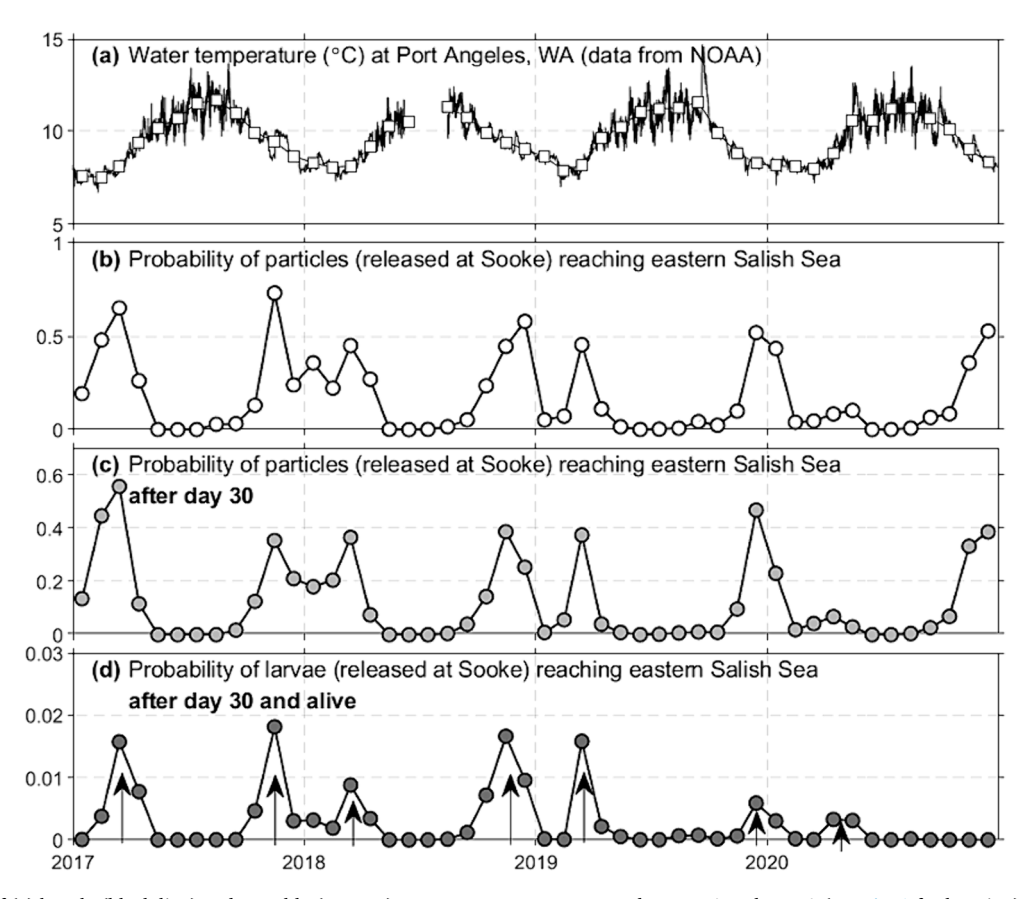


Fig. 8. Time series of (a) hourly (black line) and monthly (squares) water temperature measured at Port Angeles, WA (see Fig. 1 for location), (b) the percentage of particles from Sooke Basin reaching the eastern Salish Sea over the 4-year simulation period without considering temperature-dependent mortality or DVM, (c) the percentage of particles reaching the eastern Salish Sea at 30 days after release without considering temperature-dependent mortality or DVM, and (d) the percentage of simulated larvae reaching the eastern Salish Sea at 30 days after release when considering temperature-dependent mortality and DVM. The arrows in Panel (d) highlight the peak probability in March and November.

3.6. Impact of water temperature

The Sooke Basin release sensitivity simulations with ocean temperature artificially increased by 0.5 °C and 1 °C show doubled and quadrupled success probability of larvae from Sooke Basin intruding into the eastern Salish Sea, respectively (Fig. 14). Comparison of theses sensitivity simulations in different months indicates that the impact of water temperature change is especially notable in the seasonal transition period, e.g. in March (Fig. 14), when the low temperature is at or near the critical threshold for larval survival. The impact of artificially increased temperature is qualitatively similar for larvae released at other two sites (Figs. S7 and S8), although this impact is most pronounced for the Lummi Bay releases. Specifically, with increased water temperature, more larvae can survive to be carried northward from Lummi Bay into the northern Georgia Strait during the transition period (Fig. S8). Thus, small increases in water temperature at the transition time can dramatically enhance the survival rate of larvae and facilitate the further spread of green crabs.

4. Discussion

4.1. Transport pathways to the eastern Salish Sea

The eastern Salish Sea had presumably been somewhat protected from the invasion of green crab larvae in the past by the predominant westward current in the SJdF and the relatively cold water during seasonal flow reversals in the strait. Indeed, there is no evidence of established green crab populations within the Salish Sea (excluding Sooke Basin) prior to 2016, despite multiple years of active monitoring (Grason

et al., 2018). The recent appearance of new green crab populations in the eastern Salish Sea and its genetic connection with both the Sooke Basin and outer coastal populations (CK Tepolt, unpublished data) suggests that this transport barrier might have been breached if the invasion was facilitated by circulation-induced larval dispersal, as appears likely.

Through particle tracking modeling in the warm seasons of 2014-2016, Brasseale et al. (2018) showed that infrequent eastward flows, i.e., flow reversals, in the SJdF in spring and fall can create oceanographically favorable opportunities for green crab larvae from the outer coast and Sooke Basin to be dispersed into the eastern Salish Sea. Built upon their study, this work systematically quantifies the seasonal variation of green crab larval dispersal in the Salish Sea by i) simulating releases throughout the period of 2017–2020, ii) considering the influence of temperature-dependent mortality, and iii) diagnosing the impact of DVM. Our simulations confirms that larvae from both the outer coast and Sooke Basin populations could have been naturally carried into the eastern Salish Sea by flow reversals in the SJdF in springs and falls of 2017-2020. Meanwhile, this study provides a detailed quantification of the larval connectivity along the coast and analyzes the dispersal of green crab larvae inside the eastern Salish Sea, as well as testing the influence of future higher water temperature on patterns of dispersal.

Taken together, these modeling results support the idea that hydrodynamic connectivity is a viable pathway for larval dispersal from coastal populations to inland waters. Although conditions favorable for larvae to be advected inland from coastal locations may occur *relatively* rarely, recent growth of green crab populations in coastal embayments of Washington, such as Willapa Bay, Grays Harbor and Makah Bay, as

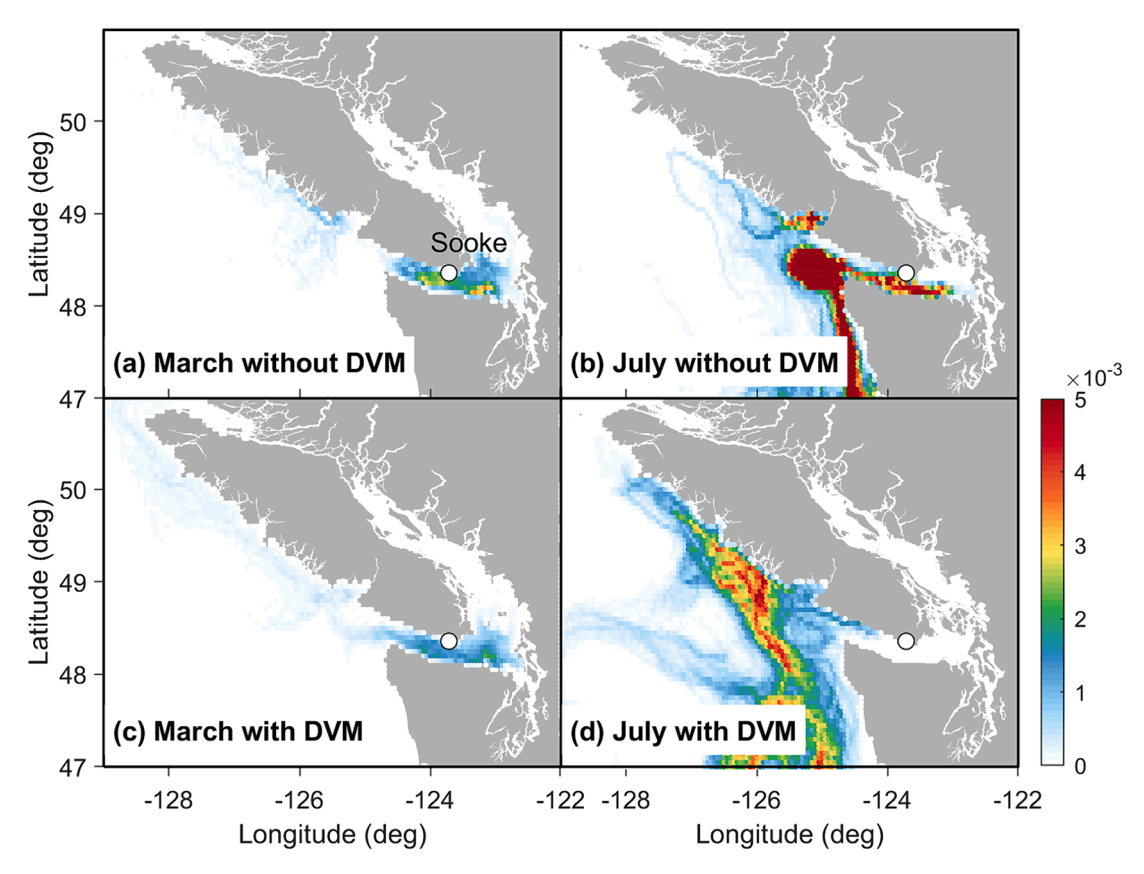


Fig. 9. Mean success probability of simulated larvae released at Sooke Basin in March (left) and July (right) of 2017 without (top) and with (bottom) DVM. Temperature-dependent mortality is included in these simulations. The release location is marked with a circle.

well as in the Sooke Basin in British Columbia (Behrens Yamada et al., 2021a, 2021b), has undoubtedly increased larval abundance in the region. Thus, propagule pressure on inland shorelines has likely increased in recent years. This is consistent with observations made by groups working to monitor and control green crab populations in the eastern Salish Sea. Despite efforts to capture and remove them, the arrival of crabs in 2016 has been followed by continuous presence in some heavily managed areas, such as Dungeness Bay on the SJdF and Drayton Harbor in the eastern Salish Sea (Washington Department of Fish and Wildlife, 2023).

Note that the majority of simulated larvae from Sooke Basin and Willapa Bay reach the eastern Salish Sea during colder months along the southern coast of SJdF (Fig. 15). Taking the March 2017 release as an example, 75 % of simulated particles from Sooke Basin and 97 % from Willapa Bay reaching the eastern Salish Sea cross the 123.5°W longitude line south of 48.25°N. This can be attributed to the relatively strong reversal flows along the southern coast in the strait (Fig. 4; Fig. 5c, 5d), which is a prominent feature in cold months. For instance, cross-strait measurements by Thomson et al. (2017) showed that the eastward reversal flow occupied the southern half of the strait with a maximum surface speed of 80 cm/s in December of 2002.

The chance of viable green crab larvae arriving in the eastern Salish Sea via flow reversals is substantially affected by water temperature. Episodic eastward flows in the SJdF typically occur in cold seasons with low water temperature that tends to limit the survival of the larvae once released. Nevertheless, during the season transition periods, particularly March and November, flow reversals coupled with warmer waters increase the likelihood of larvae released in Sooke Basin and on the outer coast arriving alive in the eastern Salish Sea within the 30–75 day window of potential developmental competence (Fig. 8). Thus, while reversals occur far less frequently during seasonal transitions than in wintertime, the former are likely much more important to delivering

larvae to the eastern Salish Sea because of higher larval survival.

4.2. Spread within the eastern Salish Sea

Of the three geographic sources of larvae modeled in this study, Lummi Bay stood out as having a substantially higher probability of influencing the eastern Salish Sea than either Willapa Bay or Sooke Basin. We note that the Lummi Bay region is chosen here as a representative eastern Salish Sea site, and the result broadly represents that the emerging populations in the eastern Salish Sea are likely most directly influencing dynamics in that region. Though perhaps not surprising, quantifying this pattern can help managers prioritize population control efforts that can help protect larger geographies. Green crab populations in the eastern Salish Sea are currently much smaller than those in either Willapa Bay or Sooke Basin, partly due to extremely intense management pressure exerted immediately after first detection of green crabs at very low densities (Washington Department of Fish and Wildlife, 2023), including by Lummi Nation biologists (Buzzell, 2023). Given the higher probability of self-recruitment in this region, particularly within the constructed sea pond in Lummi Bay (Buzzell, 2023), managers will need to sustain control pressure to keep densities relatively lower in the eastern Salish Sea. This would not only reduce the chances of rapid local population growth but also potentially hinder further spread penetrating the permeable barriers to the north (Strait of Georgia) and south (Puget Sound and Hood Canal).

4.3. Connectivity between the Salish Sea and coastal ocean

The results of this study also highlight that green crab populations within the Salish Sea (both Sooke Basin and eastern Salish Sea sites) could become a significant source of larvae for coastal embayments. This is most broadly apparent for the northern coast, but also for portions of

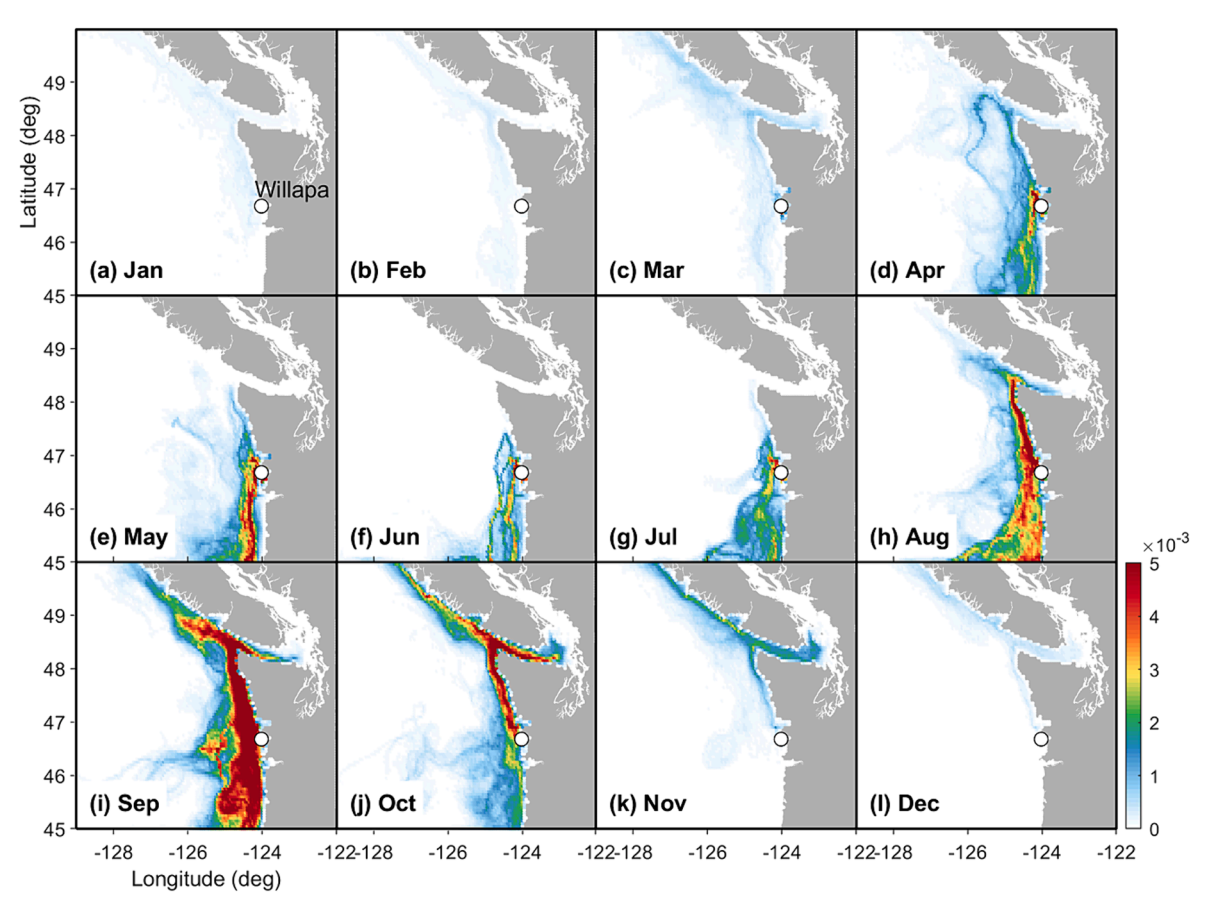


Fig. 10. Spatial distribution of monthly mean success probability of simulated larvae (with DVM and temperature-dependent mortality) being released at Willapa Bay in each month. Circles indicate the release location. Each panel shows an average over the same months in 2017–2020.

the southern coast adjacent to the SJdF, such as Makah Bay, WA, where the Makah Tribe has been working to control a growing population of green crabs since 2017. Understanding the impact of connectively on recruitment is critical to effective management throughout the region. While the lead agency in Washington State (Washington Department of Fish and Wildlife; WDFW) differentiates the Coast and Salish Sea as separate management branches, the nature of larval dispersal would suggest that action (or inaction) in one area will impact the other. Likewise, connectivity between Sooke Basin (British Columbia, Canada) and Willapa Bay (Washington, USA), underscores the importance of international management efforts outlined in the Salish Sea Transboundary Action Plan for Invasive European Green crab (Drinkwin et al., 2019).

4.4. Impact of warming

Results of our sensitivity simulations with altered water temperature (Fig. 14) suggest that, under future climate warming, the survival probability of larvae will increase, with implications for regions like the eastern Salish Sea where cold temperatures may currently limit larval success. Water temperature could also affect larval success in other ways not captured in our model, potentially amplifying or suppressing the impacts of warming demonstrated here. While our model assumes equal reproduction over time, warmer winters have historically been associated with higher reproductive output and larger cohorts of newly-recruited green crabs (Welch, 1968, Behrens Yamada et al., 2021a, 2021b). During warm periods, increased temperature will shorten the developmental time of larvae (deRivera et al., 2007), which may result in shorter dispersal distances before they need to settle onto the benthos to avoid mortality (O'Connor et al., 2007). Moreover, changes in water temperature could also result in changes to local circulation patterns,

such as the outflow of the Fraser and Skagit Rivers (Wu et al., 2012), and may thereby also alter the dispersal patterns of larvae relative to the years modeled here. The additional influence of temperature on larval success through both developmental duration/dispersal distance and oceanographic circulation patterns is likely complex and difficult to predict, but a promising area of future modeling work. Nevertheless, our simulations shed light on regions and seasons for which warming could significantly affect temperature-dependent larval mortality and resulting larval dispersal patterns. In particular, any increase in water temperature in the cold, high-mortality wintertime would exert a significant influence on the eastward expansion of green crab larvae, since the wintertime circulation in the SJdF with frequent flow reversals is more favorable for delivering larvae from either the outer coast or Sooke Basin to the eastern Salish Sea.

Analysis of the historical observational data suggests that interannual variation of water temperature in the Salish Sea can easily reach 1 °C and that this temperature change is often linked to large-scale variability, such as El Niño-Southern Oscillation (ENSO). For instance, measured water temperature at Port Angeles, WA in March shows clear interannual variation over the past two decades, and this temperature variation is closely correlated with the ENSO signal (Fig. 16). In 1998, 2015, and 2016, mean water temperature in March reached 9.5–10 °C, 1–2 °C higher than the long-term mean temperature of about 8 °C. Those anomalously high temperatures likely reflect impact of the major El Niño events in those periods. These changes in regional water temperature can presumably drive strong interannual variability in the dispersal pattern of the green crab larvae. If, during these previous years, the circulation pattern in the Salish Sea was similar to that in 2017–2020, the warmer winter conditions during those El Niño periods before 2017 could have greatly enhanced the eastward dispersal of green crab larvae. This is similar to the patterns of green crab larval

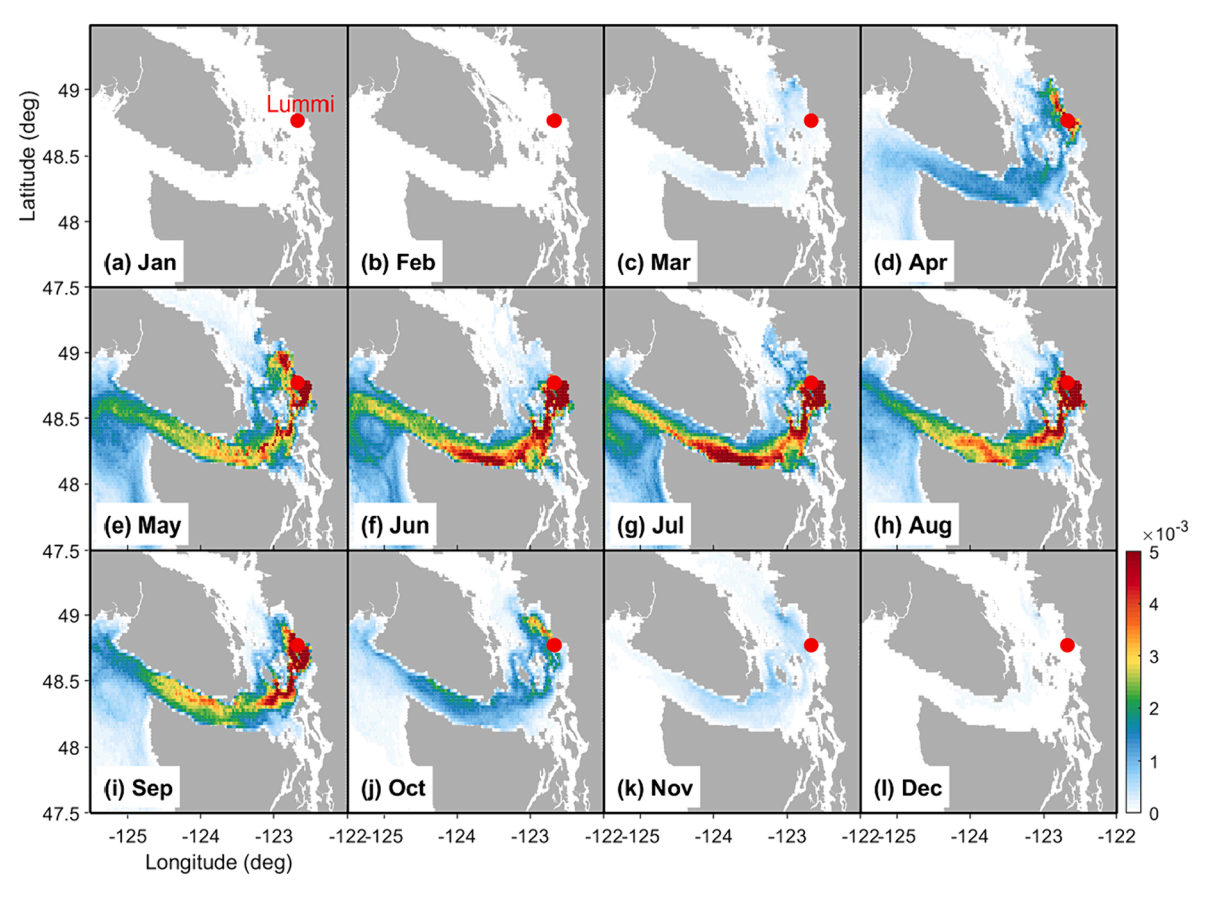


Fig. 11. Spatial distribution of mean success probability of simulated larvae released at Lummi Bay in each month. Circles indicate the release location. Each panel shows an average over the same months in 2017–2020.

dispersal observed on the outer coast (Behrens Yamada et al., 2015). Likewise, there is a growing understanding of how marine heatwaves in the eastern Pacific propagate within the Salish Sea (Khangaonkar et al., 2021). These phenomena may also result in increased water temperature and altered stratification and circulation within the region.

With a warming climate, it is anticipated that overall larval connectivity in the Salish Sea region will increase in the future. Thus, more green crab larvae from the outer coast or Sooke Basin would survive to reach the eastern Salish Sea. Warming waters may also facilitate the species' spread further north in the Strait of Georgia, as has been reported recently (Fisheries and Oceans Canada, personal communication), and more widely in the eastern Salish Sea.

4.5. Caveats and future directions

This study of the dispersal of green crab larvae in the Salish Sea is based on a number of assumptions and has limitations that could potentially be addressed in future studies. First of all, the impact of numerous factors that could play a role in green crab larval dispersal is neglected. Notably, we do not model the influence of temperature on larval developmental rate. Green crab larvae likely grow through their five larval stages in a shorter time period in warmer waters, and thus may settle out of the plankton sooner, and achieve shorter dispersal distances, than larvae in cold temperatures. Larval survival rates in our model do not consider food availability, water salinity, and probability of predation. These factors could also alter the survival rate of larvae in the ocean. In addition, successful establishment of a green crab population will also depend on post-arrival survival of juvenile and adult stages. Thus, results of our model should only be interpreted as arrival probabilities relative to possible source locations and release months.

Another limitation of this study is the assumed constant larval

release rate over time. Observations have shown that the green crab reproductive cycle has clear seasonality in larval abundance on the west coast (e.g., Banas et al., 2009; DiBacco and Therriault, 2015). Thus, the impact of seasonality in larval production should be considered in future studies to obtain a more accurate understanding of the temporal variability of green crab larval dispersal patterns in the region.

Meanwhile, for an invasive species, even a small number of founding individuals may establish a population at a new site. Therefore, small larval success probabilities matter. However, it is hard to know the exact number of larvae required or define a specific threshold of success probability for any site, as this is presumably governed by a wide range of physical and biological factors. Instead of diagnosing the exact transport pathways of green crab larvae reaching any particular sites, this study focuses on identifying the statistically most likely dispersal pathways and examining their temporal and spatial variability.

Lastly, this work examines the likelihood of *direct* transport pathways from larvae release sites to locations along the coast. In the ocean, larvae can also be transported to a site through multi-year and multi-generation *indirect* pathways via a leapfrog pattern (*sensu* Grosholz and Ruiz. 1995) with intermediate cryptic populations developing along the way. The likelihood of such indirect pathways should be considered in future studies to diagnose the exact mechanisms of green crab larval dispersal into the eastern Salish Sea.

5. Conclusions and implications for management

Results of our simulations highlight strong seasonality in green crab larval dispersal in the Salish Sea, resulting from seasonal variation in the regional ocean circulation, particularly in the SJdF. These simulations identify a possible direct transport pathway during a narrow time window for green crab larvae to spread into the eastern Salish Sea from

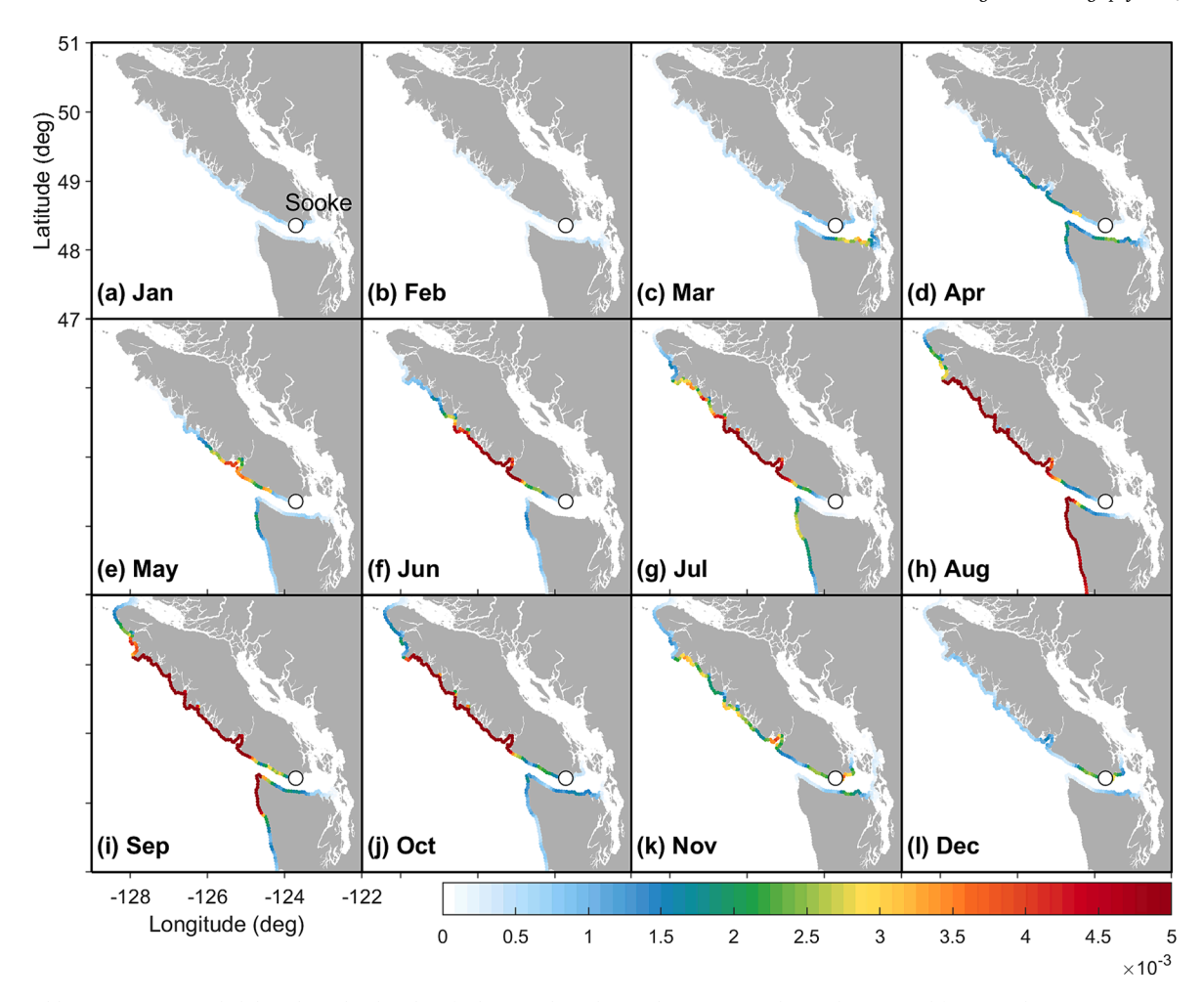


Fig. 12. Monthly mean success probability along the shoreline for larvae released at Sooke Basin in each month computed from simulations over 2017–2020. A total of 544 sample locations along the shoreline are plotted. The circle in each panel denotes the location of Sooke Basin.

coastal ocean sources and Sooke Basin. In particular, frequent surface current reversals in the SJdF in the cold season can carry a substantial number of larvae from the outer coast and Sooke Basin eastward into the eastern Salish Sea. However, survival is likely low because of unfavorable wintertime temperatures. During seasonal transition periods, notably March and November, the water temperature is slightly above the critical threshold of larval survival, which allows a small proportion of larvae released in those months to survive and reach the inner coast in the eastern Salish Sea. Meanwhile, larvae released from the newlyestablished eastern Salish Sea populations may quickly spread to nearby areas, particularly to the immediate north, and can also be carried to the SJdF and outer coast by the predominant westward current in the warm seasons. Notably, this spread is bounded: model simulations suggest that the connectivity of the eastern Salish Sea with northern Georgia Strait in 2017-2020 was low, presumably due to predominant flows in the region suppressing the spread of larvae to the region farther north. Our simulations also suggest that this type of hydrodynamic barrier is permeable. Temporal variation of the circulation pattern, even over short periods of time, may lead to drastically different larval dispersal patterns, as demonstrated by the influence of flow reversals in

Patterns of simulated larval dispersal are strongly influenced by water temperature, owing to temperature-dependent mortality. Our sensitivity simulations with altered water temperature suggest that, if regional circulation remains the same, an increase in the water temperature by only 0.5–1 $^{\circ}\mathrm{C}$ could result in a much more extensive spread of this damaging invasive species in the eastern Salish Sea and higher

exchange between populations in the region. Large-scale oceanic and atmospheric processes, such as ENSO, already induce temperature change in the region of this magnitude over interannual time scales, and future climate change is predicted to result in a gradual increase in the water temperature in the Salish Sea region. Yet, ocean warming will likely influence oceanography and green crab development through a range of complex interactions not captured by this model, and the precise ways in which large-scale processes could affect larval dispersal in the Salish Sea remains unknown. The present study demonstrates that local hydrodynamic processes could play a major role in the spread of invasive green crabs in the Salish Sea region, and the interaction between the local and large-scale oceanographic and climate processes should be considered for effective coastal resource management and efficient conservation efforts.

Changing ocean conditions may complicate extrapolating model results into the future. Nevertheless, this study supports management by broadening our understanding of how variability in regional oceanographic processes can influence green crab recruitment, which could aid in decision-making. For instance, when oceanographic data are available in near real-time, managers could focus on detecting instances when current reversals coincide with suitable temperatures, and planning for additional control efforts targeted at the impacted regions during subsequent months. By considering the temporal and geographic contexts that affect larval success, managers can make better and more timely assessments of resource needs and control effort priorities, and choose to target effort at locations and times having relatively large impact.

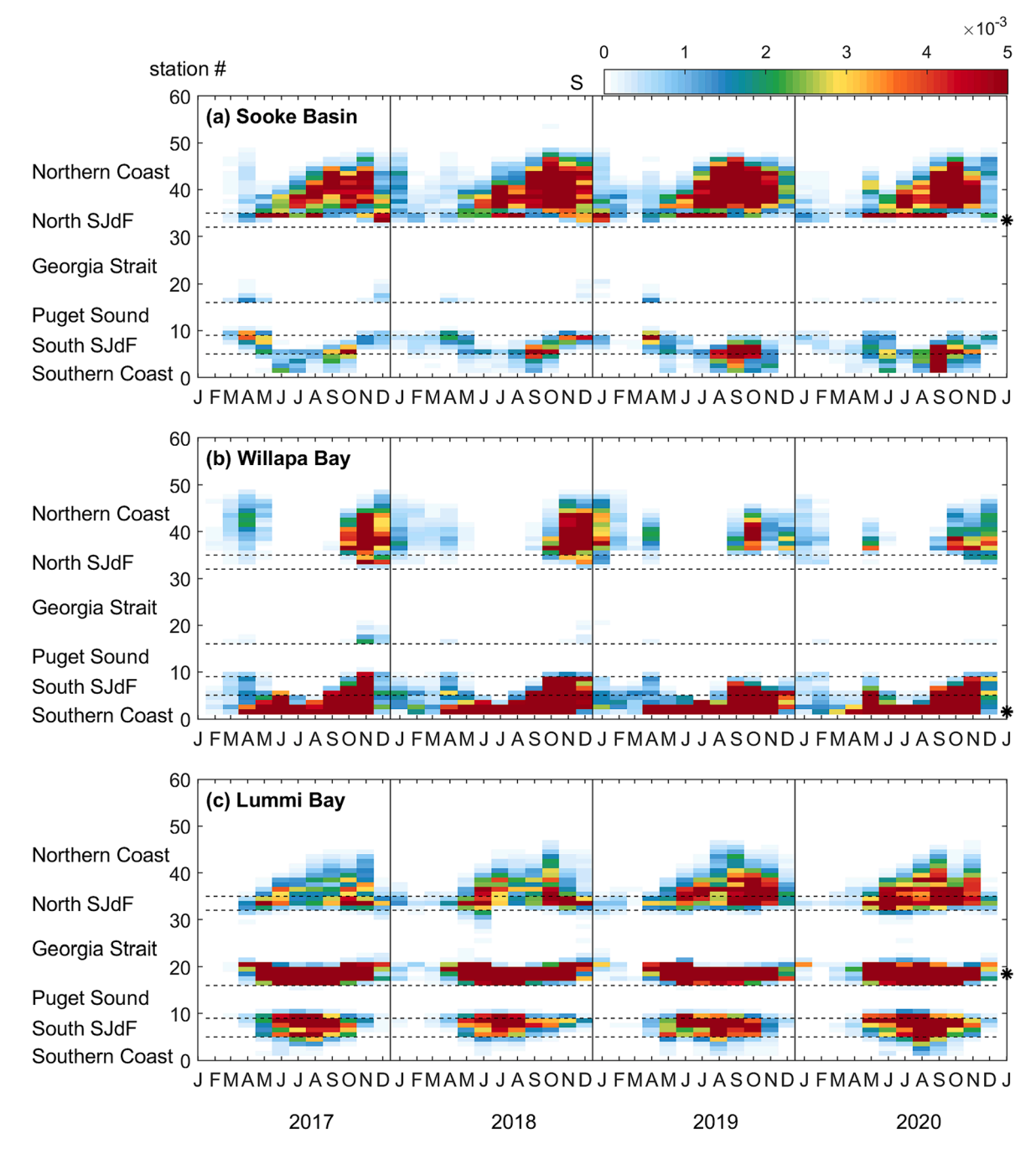


Fig. 13. Temporal and along-shoreline variation of the mean success probability index of larvae released at (a) Sooke Basin, (b) Willapa Bay, and (c) Lummi Bay at 54 major sampling stations. The thin dashed lines highlight the mouth of the SJdF, and the asterisks to the right of the panels indicate the three release locations.

Data availability Statement

The LiveOcean model output are available at https://faculty.washington.edu/pmacc/LO/LiveOcean.html. The ROMSPath model code is available at https://github.com/imcslatte/ROMSPath.git. The ENSO index is publicly available at https://psl.noaa.gov/enso/mei/. The NOAA tidal gauge data are available at https://tidesandcurrents.noaa.gov/stationhome.html?id=9444090.

CRediT authorship contribution statement

Jiabi Du: Writing – original draft, Visualization, Validation, Methodology, Investigation, Formal analysis, Data curation, Conceptualization. **Carolyn K. Tepolt:** Writing – review & editing, Project

administration, Funding acquisition, Conceptualization. **Emily W. Grason:** Writing – review & editing, Validation, Funding acquisition, Data curation, Conceptualization. **P. Sean McDonald:** Writing – review & editing, Investigation, Funding acquisition, Conceptualization. **Yan Jia:** Writing – review & editing, Visualization, Methodology. **Weifeng G. Zhang:** Writing – review & editing, Visualization, Validation, Supervision, Software, Resources, Project administration, Methodology, Investigation, Funding acquisition, Formal analysis, Data curation, Conceptualization.

Declaration of competing interest

The authors declare that they have no known competing financial interests or personal relationships that could have appeared to influence

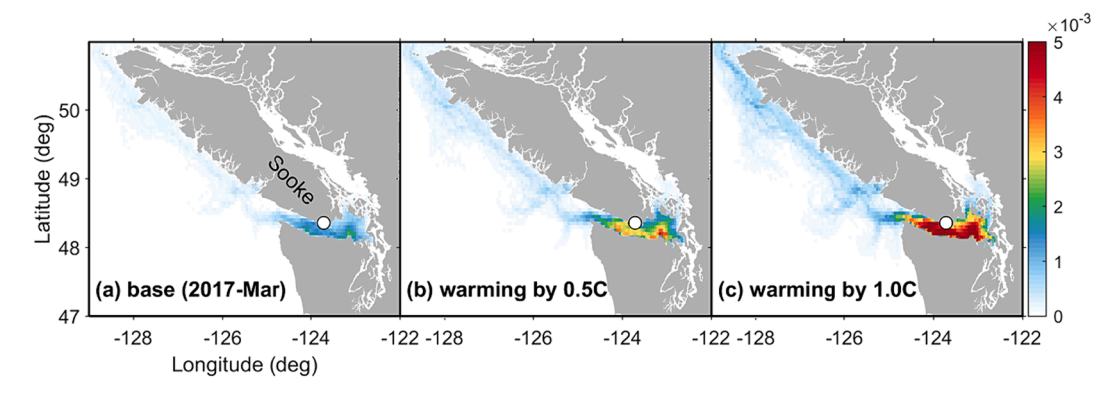


Fig. 14. Success probability of larvae released in Sooke Basin under different conditions: (a) baseline condition in March 2017, and uniformly increased water temperature from the March 2017 condition by (b) 0.5 °C and (c) 1° C. The circle in each panel denotes the location of Sooke Basin.

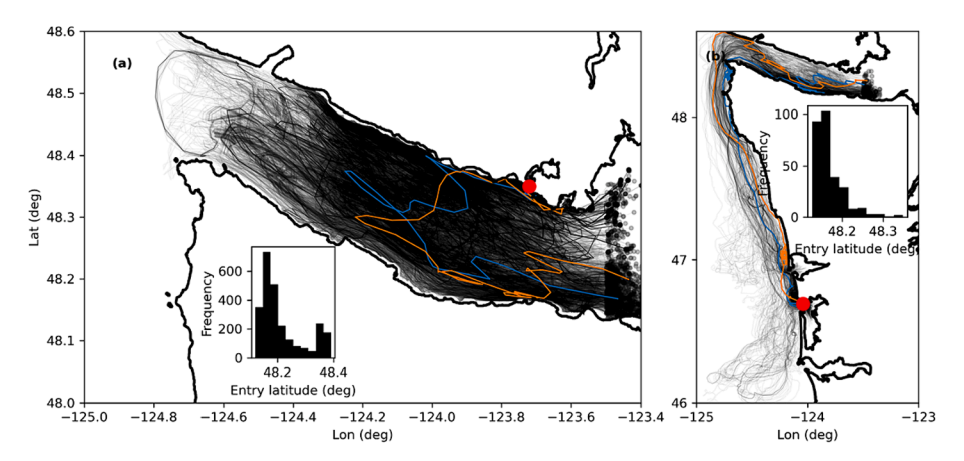


Fig. 15. Tracks of particles released at (a) Sooke Basin and (b) Willapa Bay in March 2017 reaching the eastern Salish Sea (defined here as crossing the 123.5°W longitude line). In each panel, the thin gray lines are tracks of individual particles; black thick line is the coastline; the red dot indicates the release location; gray dots at the east end of the track indicate the location where particles enter the eastern Salish Sea; orange and blue lines are the tracks of two selected particles. The inset in each panel demonstrates the distribution of particle entry locations. (For interpretation of the references to color in this figure legend, the reader is referred to the web version of this article.)

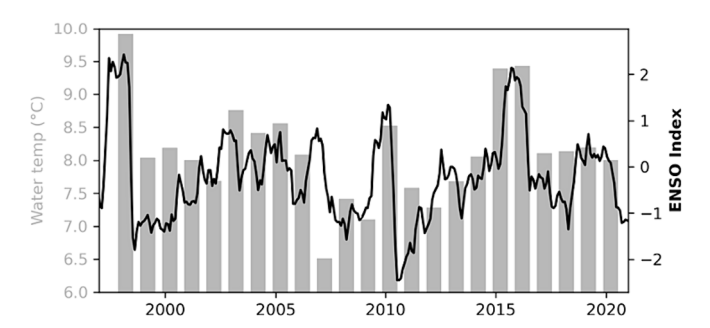


Fig. 16. Observed mean water temperature in March (gray bar) at Port Angeles, WA (NOAA tidal gauge station 9444090) and the ENSO index (black line) over 1998–2020.

the work reported in this paper.

Data availability

We have shared the links to the data in the Data Availability Statement of the submitted manuscript.

Acknowledgements

We thank Dr. Parker MacCready for sharing the LiveOcean model

output. This study was financially supported by the National Science Foundation (award OCE-1850996) and Washington State via Governor Jay Inslee, the State Legislature, and the Washington Department of Fish and Wildlife.

Appendix A. Supplementary data

Supplementary data to this article can be found online at https://doi.org/10.1016/j.pocean.2024.103245.

References

Álvarez-Noriega, M., Burgess, S.C., Byers, J.E., Pringle, J.M., Wares, J.P., Marshall, D.J., 2020. Global biogeography of marine dispersal potential. Nat. Ecol. Evol. 4 (9), 1196–1203. https://doi.org/10.1038/s41559-020-1238-y.

Banas, N.S., Mcdonald, P.S., Armstrong, D.A., 2009. Green crab larval retention in Willapa Bay, Washington: an intensive Lagrangian modeling approach. Estuar. Coasts 32 (5), 893–905. https://doi.org/10.1007/s12237-009-9175-7.

Behrens Yamada, S., Kosro, P.M., 2010. Linking ocean conditions to year class strength of the invasive European green crab *Carcinus maenas*. Biol. Invasions 12 (6), 1791–1804. https://doi.org/10.1007/s10530-009-9589-y.

Behrens Yamada, S., Peterson, W.P., Kosro, P.M., 2015. Biological and physical ocean indicators predict the success of an invasive crab, *Carcinus maenas*, in the northern California current. Mar. Ecol. Prog. Ser. 537, 175–189. https://doi.org/10.3354/ meps11431.

Behrens Yamada, S., Thomson, R.E., Gillespie, G.E., Norgard, T.C., 2017. Lifting Barriers to Range Expansion: the European Green Crab Carcinus maenas (Linnaeus, 1758) Enters the Salish Sea. J. Shellfish. Res. 36 (1), 201–208. https://doi.org/10.2983/ 035.036.0121.

Behrens Yamada, S., Fisher, J.L., Kosro, P.M., 2021a. Relationship between ocean ecosystem indicators and year class strength of the invasive European green crab

- (Carcinus maenas). Prog. Oceanogr. 196, 102618 https://doi.org/10.1016/j.
- Behrens Yamada, S., Gillespie, G.E., Thomson, R.E., Norgard, T.C., 2021b. Ocean indicators predict range expansion of an introduced species: invasion history of the European green crab *Carcinus maenas* on the North American Pacific coast. J. Shellfish. Res. 40 (2), 399–413. https://doi.org/10.2983/035.040.0212.
- Berrill, M., 1982. The life cycle of the green crab *Carcinus maenas* at the northern end of its range. J. Crustac. Biol. 2 (1), 31–39. https://doi.org/10.2307/1548108.
- Brasseale, E., Grason, E.W., McDonald, P.S., Adams, J., MacCready, P., 2019. Larval transport modeling support for identifying population sources of European green crab in the Salish Sea. Estuar. Coasts 42 (6), 1586–1599. https://doi.org/10.1007/ s12237-019-00586-2.
- Buzzell, B., 2023. The 2021 European green crab (Carcinus maenas) invasion in Lummi Sea Pond. Aquatic Invasive Species Division Technical Report. Lummi Natural Resources Department, Bellingham, Washington, pp. 27+v.
- Cannon, G.A., 1978. Circulation in the Strait of Juan de Fuca: Some recent oceanographic observations (NOAA Tech. Rep. ERL 399-PMEL 29). National Oceanic and Atmospheric Administration, Seattle, WA.
- Carlton, J.T., Cohen, A.N., 2003. Episodic global dispersal in shallow water marine organisms: the case history of the European shore crabs *Carcinus maenas* and *C. aestuarii. J. Biogeogr.* 30 (12), 1809–1820. https://doi.org/10.1111/j.1365-2699 2003 00960 x
- Cohen, A.N., Carlton, J.T., Fountain, M.C., 1995. Introduction, dispersal and potential impacts of the green crab *Carcinus maenas* in San Francisco Bay. California. *Marine Biology* 122 (2), 225–237. https://doi.org/10.1007/BF00348935.
- Cowen, R.K., Sponaugle, S., 2009. Larval dispersal and marine population connectivity. Ann. Rev. Mar. Sci. 1 (1), 443–466.
- Curtis, L.J.F., Curtis, D.L., Matkin, H., Thompson, M., Choi, F., Callow, P., et al., 2015. Evaluating transfers of harvested shellfish products, from the west to the east coast of Vancouver Island, as a potential vector for European Green Crab (Carcinus maenas) and other non-indigenous invertebrate species. Canadian Science Advisory Secretariat.
- deRivera, C.E., Hitchcock, N.G., Teck, S.J., Steves, B.P., Hines, A.H., Ruiz, G.M., 2007. Larval development rate predicts range expansion of an introduced crab. Mar. Biol. 150 (6), 1275–1288. https://doi.org/10.1007/s00227-006-0451-9.
- DiBacco, C., Therriault, T.W., 2015. Reproductive periodicity and larval vertical migration behavior of European green crab *Carcinus maenas* in a non-native habitat. Mar. Ecol. Prog. Ser. 536, 123–134. https://doi.org/10.3354/meps11422.
- Drinkwin, J., Pleus, A., Therriault, T., Talbot, R., Grason, E.W., McDonald, P.S., Adams, J., Hass, T., Litle, K., 2019. Salish Sea Transboundary Action Plan for Invasive European Green Crab. Puget Sound Partnership.
- Ens, N.J., Harvey, B., Davies, M.M., Thomson, H.M., Meyers, K.J., Yakimishyn, J., et al., 2022. The Green Wave: reviewing the environmental impacts of the invasive European green crab (*Carcinus maenas*) and potential management approaches. Environ. Rev. 30 (2), 306–322. https://doi.org/10.1139/er-2021-0059.
- Frisch, A.S., Holbrook, J., Ages, A.B., 1981. Observations of a summertime reversal in circulation in the Strait of Juan De Fuca. J. Geophys. Res. Oceans 86 (C3), 2044–2048. https://doi.org/10.1029/JC086iC03p02044.
- Giddings, S.N., MacCready, P., Hickey, B.M., Banas, N.S., Davis, K.A., Siedlecki, S.A., Trainer, V.L., Kudela, R.M., Pelland, N.A., Connolly, T.P., 2014. Hindcasts of potential harmful algal bloom transport pathways on the Pacific Northwest coast. J. Geophys. Res. Oceans 119 (4), 2439–2461. https://doi.org/10.1002/ 2013JC009622.
- Giddings, S.N., MacCready, P., 2017. Reverse estuarine circulation due to local and remote wind forcing, enhanced by the presence of along-coast estuaries. J. Geophys. Res. Oceans 122 (12), 10184–10205. https://doi.org/10.1002/2016JC012479.
- Grason, E., McDonald, S., Adams, J., Litle, K., Apple, J., Pleus, A., 2018. Citizen science program detects range expansion of the globally invasive European green crab in Washington State (USA). Management of Biological Invasions 9 (1), 39–47. https:// doi.org/10.3391/mbi.2018.9.1.04.
- Grosholz, E.D., Ruiz, G.M., 1995. Spread and potential impact of the recently introduced European green crab, *Carcinus maenas*, in central California. Mar. Biol. 122 (2), 239–247. https://doi.org/10.1007/BF00348936.
- Hickey, B.M., McCabe, R., Geier, S., Dever, E., Kachel, N., 2009. Three interacting freshwater plumes in the northern California Current System. J. Geophys. Res. 114, C00B03. https://doi.org/10.1029/2008JC004907.
- Hidalgo, F.J., Barón, P.J., Orensanz, J.M. (Lobo), 2005. A prediction come true: the green crab invades the Patagonian coast. Biol. Invasions 7 (3), 547–552. https://doi.org/ 10.1007/s10530-004-5452-3
- Holbrook, J.R., Halpern, D., 1982. Winter-time near-surface currents in the strait of Juan de Fuca. Atmos. Ocean 20 (4), 327–339. https://doi.org/10.1080/ 07055900.1982.9649149.
- Holbrook, J.R., Meunch, R.D., Kachel, D.G., Wright, C., 1980. Circulation in the Strait of Juan de Fuca: Recent Oceanographic Observations in the Eastern Basin (NOAA Tech. Rep. ERL 412-PMEL 33). National Oceanic and Atmospheric Administration, Seattle, WA

- Hunter, E.J., Fuchs, H.L., Wilkin, J.L., Gerbi, G.P., Chant, R.J., Garwood, J.C., 2022. ROMSPath v1.0: offline particle tracking for the Regional Ocean Modeling System (ROMS). Geosci. Model Dev. 15 (11), 4297–4311. https://doi.org/10.5194/gmd-15-4297-2022
- Huyer, A., Sobey, E.J.C., Smith, R.L., 1979. The spring transition in currents over the Oregon Continental Shelf. J. Geophys. Res. Oceans 84 (C11), 6995–7011. https://doi.org/10.1029/JC084iC11p06995.
- Keller, A.G., Grason, E.W., McDonald, P.S., Ramón-Laca, A., Kelly, R.P., 2022. Tracking an invasion front with environmental DNA. Ecol. Appl. 32 (4), e2561.
- Khangaonkar, T., Nugraha, A., Yun, S.K., Premathilake, L., Keister, J.E., Bos, J., 2021. Propagation of the 2014–2016 Northeast Pacific marine heatwave through the Salish Sea. Front. Mar. Sci 8, 787604. https://doi.org/10.3389/fmars.2021.787604.
- Kinlan, B.P., Gaines, S.D., 2003. Propagule dispersal in marine and terrestrial environments: a community perspective. Ecology 84 (8), 2007–2020. https://doi. org/10.1890/01-0622.
- Kinlan, B.P., Gaines, S.D., Lester, S.E., 2005. Propagule dispersal and the scales of marine community process. Divers. Distrib. 11, 139–148.
- Klassen, G., Locke, A., 2007. A biological synopsis of the European green crab, Carcinus maenas. Can. Manuscr. Rep. Fish. Aquat. Sci. 1488–5387, 2818.
- MacCready, P., McCabe, R.M., Siedlecki, S.A., Lorenz, M., Giddings, S.N., Bos, J., et al., 2021. Estuarine circulation, mixing, and residence times in the Salish Sea. J. Geophys. Res. Oceans 126 (2), e2020JC016738. https://doi.org/10.1029/ 2020JC016738.
- Moore, S.K., Johnstone, J.A., Banas, N.S., Salathé, E.P., 2015. Present-day and future climate pathways affecting Alexandrium blooms in Puget Sound. WA, USA, Harmful Algae 48, 1–11. https://doi.org/10.1016/j.hal.2015.06.008.
- Morgan, S., Dibble, C., Susner, M., Wolcott, T., Wolcott, D., Largier, J., 2021. Robotic biomimicry demonstrates behavioral control of planktonic dispersal in the sea. Mar. Ecol. Prog. Ser. 663, 51–61. https://doi.org/10.3354/meps13635.
- Nakicenovic, N., Alcamo, J., Davis, G., Vries, B.D., Fenhann, J., Gaffin, S., Gregory, K., Grübler, A., Jung, T.Y., Kram, T., Rovere, E.L.L., Michaelis, L., Mori, S., Morita, T., Pepper, W., Pitcher, H., Price, L., Riahi, K., Roehrl, A., Rogner, H.-H., Sankovski, A., Schlesinger, M., Shukla, P., Smith, S., Swart, R., Rooijen, S.V., Victor, N., Dadi, Z., 2000. IPCC Special Report on Emissions Scenarios. Cambridge University Press.
- Nils, 2023. Scatter Plot colored by Kernel Density Estimate. https://www.mathworks.com/matlabcentral/fileexchange/65728-scatter-plot-colored-by-kernel-density-estimate, MATLAB Central File Exchange. Retrieved August 25, 2023.
- O'Connor, M.I.O., Bruno, J.F., Gaines, S.D., Halpern, B.S., Lester, S.E., Kinlan, B.P., Weiss, J.M., 2007. Temperature control of larval dispersal and the implications for marine ecology, evolution, and conservation. Proc. Natl. Acad. Sci. USA 104 (4), 1–6. https://doi.org/10.1073/pnas.0603422104.
- Palumbi, S.R., Pinsky, M., 2014. Marine dispersal, ecology, and conservation. In: Bertness, M., Bruno, J., Silliman, B., Stachowicz, J. (Eds.), Marine Community Ecology and Conservation, first ed. Sinauer Associates, pp. 57–84.
- Queiroga, H., Blanton, J., 2005. Interactions between behaviour and physical forcing in the control of horizontal transport of decapod crustacean larvae. Adv. Mar. Biol. 47, 107–214. https://doi.org/10.1016/s0065-2881(04)47002-3.
- Shchepetkin, A.F., McWilliams, J.C., 2005. The regional oceanic modeling system (ROMS): a split-explicit, free-surface, topography-following-coordinate oceanic model. Ocean Model. 9 (4), 347–404. https://doi.org/10.1016/j. ocemod.2004.08.002.
- Tepolt, C.K., 2023. Thermal Biology. In: Weihrauch, D., Mcgaw, I. (Eds.), Ecophysiology of the European Green Crab (Carcinus maenas) and Related Species, first ed.,. Elsevier, pp. 231–247.
- Thomson, R.E., 1981. Oceanography of the British Columbia Coast. Canadian Special Publication of Fisheries and Aquatic Sciences, Ottawa, Canada, p. 291.
- Thomson, R.E., Mihály, S.F., Kulikov, E.A., 2007. Estuarine versus transient flow regimes in Juan de Fuca Strait. J. Geophys. Res. Oceans 112 (C9). https://doi.org/10.1029/ 2006JC003925.
- Vaughn, D., Allen, J.D., 2010. The peril of the plankton. Integr. Comp. Biol. 50 (4), 552–570. https://doi.org/10.1093/icb/icq037.
- Visser, A.W., 1997. Using random walk models to simulate the vertical distribution of particles in a turbulentwater column. Mar. Ecol. Prog. Ser. 158, 275–281. https:// doi.org/10.3354/meps158275.
- Washington Department of Fish and Wildlife, 2023, European Green Crab quarterly progress report Fall 2023 (July 1 to September 30, 2023), https://wdfw.wa.gov/sites/default/files/publications/02460/wdfw02460.pdf.
- Weihrauch, D., McGaw, I., 2023. In: Ecophysiology of the European Green Crab (Carcinus maenas) and Related Species: Mechanisms Behind the Success of a Global Invader, first ed. Elsevier, p. 289.
- Welch, W.R., 1968. Changes in abundance of the green crab, Carcinus maenas (L.), in relation to recent temperature changes. Fish. Bull. 67, 337–345.
- Wu, H., Kimball, J.S., Elsner, M.M., Mantua, N., Adler, R.F., Stanford, J., 2012. Projected climate change impacts on the hydrology and temperature of Pacific Northwest rivers. Water Resour. Res. 48 (11) https://doi.org/10.1029/2012WR012082.